

Chapter 2

Propagation of Elastic Waves in Solids

Elasticity is a solid's most important property for restoring its shape and volume after the termination of the action of the external forces applied to it, while for liquids and gases, only volume is restored. Therefore the medium, whose typical feature is elasticity, is referred to as “elastic medium.” Accordingly, *elastic vibrations* are vibrations of mechanical systems, elastic medium, or its part that arises under mechanical disturbances. *Elastic* or *acoustic waves* are mechanical disturbances that reproduce in an elastic medium. A partial case of acoustic waves is a sound, which is audible to man; thus the term “acoustics” (from the Greek “*akustikos*,” which means “auditory”) was given to this phenomenon. In the widest sense, acoustics involves the study of elastic waves, and in the narrowest, it is often used to define their sound range only.

Elastic vibrations and acoustic waves are widely used in nondestructive testing and technical diagnostics of materials and products, in various engineering devices and equipment. For example, powerful ultrasonic vibrations are used for the local fracture of brittle high-strength materials (ultrasonic crushing); dispersion (fine crushing of solid or liquid bodies in any medium—for example, fats in water); coagulation (enlargement of particles of a substance, such as smoke); and for other purposes. Elastic vibrations and waves are very important for the investigation of the processes of initiation and propagation of the volume damaging and fracture of solids; this is what has made it possible to use them widely in fundamental and applied scientific studies of these processes from the viewpoint of fracture mechanics.

2.1 Types of Elastic Waves

2.1.1 Some General Ideas on Elastic Strain

Elastic vibrations in liquids and gases are characterized by one of the following parameters: change in pressure p or density ρ ; particle shift from an equilibrium

state \mathbf{u} ; vibration motion velocity \mathbf{v} ; or shear potential χ , i.e., vibration velocity ϕ . It is essential to distinguish the change in pressure or density caused by acoustic wave propagation from their statistical (average) value. All the above-mentioned parameters are interconnected, for example: $\mathbf{u} = \text{grad}\chi$; $\mathbf{v} = \text{grad}\phi$; $\mathbf{v} = \partial\mathbf{u}/\partial t$; $p = \rho\partial\phi/\partial t$, where ρ is the medium density, and t is the time [1].

Unlike liquids and gases, the acoustic field in a solid is of a more complicated nature, because a solid possesses not only the volume elasticity as liquids and gases do, but also the elasticity of their shape, i.e., shear elasticity. The concept of stress is introduced for solids instead of pressure, i.e., the force related to a surface unit.

In the mechanics of a deformed solid there are normal (tensile or compressive) σ_{xx} , σ_{yy} , σ_{zz} and tangent or tangential (shear) σ_{xy} , σ_{yz} stresses, etc. In general, the stress state of a solid is characterized by a third-rank tensor σ_{ij} , where indices i and j take the values of coordinate axes x , y , z . The first index indicates the coordinate toward which the force acts, and the second index defines the plane perpendicular to the direction of the coordinate indicated by the second index, to which this force is applied. This tensor is symmetric, i.e., $\sigma_{ij} = \sigma_{ji}$.

Since in liquids and gases there is no elasticity in a shape, there are no tangential components of a stress tensor, and normal components are equal to each other and to a pressure with a reverse sign. The pressure is negative when it creates tensile stresses that are considered to be positive; on the contrary, pressure is assumed to be with a plus when it creates compressing stresses.

A typical feature of vibrations in a solid is the change in stresses σ_{ij} , displacement of its particles u_i and shear potential. The concept of vibration velocity is rarely used. More often, vibrations are characterized by deformation (“*deformation*” in Latin means “distortion”), i.e., the change in mutual location ∂u of the body points. This change is compared to the primary distance between points; as a result, the deformation is a dimensionless quantity. If points are displaced along a segment connecting them, the tension-compression deformation occurs in a solid, and if they are displaced perpendicular to this segment direction, we have a shear deformation, which is why the deformation is written as a tensor ε_{ij} , similar to a stress tensor. Herein, $\varepsilon_{xx} = \partial u_x/\partial x$ is the tension-compression deformation along the x axis. For the symmetry of strain tensor, its components are written as $\varepsilon_{xy} = (\partial u_x/\partial y + \partial u_y/\partial x)/2$. Other shear components of deformation are written similarly. The value of $\varepsilon = \varepsilon_{xx} + \varepsilon_{yy} + \varepsilon_{zz}$ implies the change of the volume $dx dy dz$ of an elementary cube. For liquids and gases, there are no shear deformations while the tension-compression deformations are the same in all directions.

In this chapter we consider an isotropic medium only. Isotropy (from the Greek “*isos*”, which means “equal” or “identical,” and “*tropos*,” which means “direction”) means that physical properties of a medium do not depend on the direction chosen in it. Media, whose properties depend on the direction, are called “anisotropic” (from the Greek “*anisos*,” which means “unequal”).

Hook’s law relates a proportional dependence between stresses and strains. In a generalized form, it looks like

$$\sigma_{ij} = \delta_{ij}\Lambda\varepsilon_{ii} + 2\mu\varepsilon_{ij}, \quad (2.1)$$

where $\delta_{ij} = 1$, if $i = j$, and $\delta = 0$, for $i \neq j$; Λ and μ are Lamé constants. In engineering practice, instead of the latter, the modules of the normal elasticity E and shear G are used. They are related by the following dependence [2]:

$$E = \mu(3\Lambda + 2\mu)/(\Lambda + \mu), \quad G = \mu. \quad (2.2)$$

Alongside these modules, another important elastic constant, i.e., the Poisson's ratio ν , is also used in calculations. It is defined as the ratio of compression to elongation of the tensioned bar:

$$\nu = \frac{\Lambda}{2(\Lambda + \mu)} = \frac{E}{2G} - 1. \quad (2.3)$$

In all cases, a couple of independent elastic constants characterize the elastic properties of an isotropic solid.

2.1.2 A Wave Equation for a Solid

It is derived by using the second Newton's law for an elementary volume $dxdydz$. The difference of forces applied to its opposite faces is equated to the product of mass and acceleration. As a result, we get for axis x

$$\rho \frac{\partial^2 u_x}{\partial t^2} = \frac{\partial \sigma_{xx}}{\partial x} + \frac{\partial \sigma_{xy}}{\partial y} + \frac{\partial \sigma_{xz}}{\partial z}. \quad (2.4)$$

By analogy, it is possible to write the equation for axes y and z .

By substituting strains from (2.1) instead of stresses, the equation of wave propagation in an elastic medium is obtained:

$$\rho \frac{\partial^2 u_x}{\partial t^2} - (\Lambda + \mu) \frac{\partial \varepsilon}{\partial x} - \mu \nabla^2 u_x = 0, \quad (2.5)$$

where $\nabla^2 = \partial^2 / \partial x^2 + \partial^2 / \partial y^2 + \partial^2 / \partial z^2$ is the Laplace operator. The wave equations (2.5) include second-order time, and coordinate derivatives with different signs with respect to some variable. Using a vector analysis, the equation of (2.5) type for all coordinates can be written as one expression:

$$\rho \frac{\partial^2 \mathbf{u}}{\partial t^2} = (\Lambda + \mu) \text{grad div } \mathbf{u} + \mu \nabla^2 \mathbf{u}. \quad (2.6)$$

When $\mu = 0$, and assuming the displacement $u_x = u_y = u_z = u$ to be the same in all directions (scalar), Eq. (2.6) is transformed to a wave equation for a liquid or a gas:

$$\frac{\partial^2 \mathbf{u}}{\partial t^2} = c^2 \nabla^2 u, \quad (2.7)$$

where $c = \sqrt{\Lambda/\rho}$ is the velocity of propagation of elastic waves. The same equations are valid for other elastic values, i.e., pressure, potential, etc.

2.1.3 Main Ideas of the Wave Process

The solution of Eq. (2.7) for the potential of velocity:

$$\frac{\partial^2 \varphi}{\partial t^2} = c^2 \nabla^2 \varphi. \quad (2.8)$$

Displacements and vibration velocities for liquids and gases are the same in all directions, so they can be considered to be scalars u and v . For simplicity, assume that function φ depends only on the coordinate x : $\nabla^2 \varphi = \partial^2 \varphi / \partial x^2$. It is known from the theory of differential equations in partial derivatives that the solution of such an equation looks like $\varphi = \varphi_1(x - ct) + \varphi_2(x + ct)$, where φ_1 and φ_2 are arbitrary functions that are differentiated twice. The first element is a wave that propagates along the x axis in the positive direction, and the second is a wave that propagates in the opposite direction. Hereinafter, as a rule, we will take into consideration a direct wave and will omit the second term; therefore, before t there should be a minus if there is a plus before x .

In the case of harmonic wave propagation, we can write (2.9):

$$\varphi = \varphi_1 = \Phi \cos \left[\frac{\omega}{c} (x - ct) \right] = \Phi \cos(kx - \omega t). \quad (2.9)$$

Here, Φ is the amplitude, $kx - \omega t$ is the phase, $\omega = 2\pi f$ is the circular frequency, f is the vibration frequency, $T = 1/f$ is the period of vibrations, $k = \omega/c = 2\pi/\lambda$ is the wave number, and λ is the wavelength, i.e., the distance that a wave passes for a period of vibrations. If t changes by a period or x changes by a wavelength, a phase will change by 2π , and consequently the cosine value will be the same.

The other harmonic wave presentation is

$$\varphi = \text{Re} \left[\Phi e^{j(kx - \omega t)} \right], \quad (2.10)$$

where $j = \sqrt{-1}$. Symbol Re indicates that the real part of the complex function, which is in square brackets, is taken. Since $e^{ja} = \cos a + j \sin a$, expressions (2.9) and (2.10) coincide. The Re sign is not usually written, but it is actually implied.

In a plane, perpendicular to the x axis, the wave phase is the same (this plane is a wave front). A wave with a plane front is called a “plane wave,” and a direction perpendicular to the front is called a “ray.”

The harmonic plane wave of an arbitrary direction can be written as [3]:

$$\varphi = \Phi e^{j(\mathbf{k}\mathbf{r} - \omega t)}. \quad (2.11)$$

Here, $\mathbf{k}\mathbf{r} = k_x x + k_y y + k_z z$ is a scalar product of the radius-vector of a point in space \mathbf{r} and the vector $\mathbf{k} = \mathbf{n}\omega/c$, where \mathbf{n} is a unit vector that characterizes a wave direction, and k_x, k_y, k_z are vector components. For a plane wave that propagates along an x axis, we have $k_x = k$; $k_y = k_z = 0$; as a result, we get a formula (2.10).

For the harmonic (or monochromatic) plane waves mentioned above, i.e., the waves that have one frequency of vibrations and an infinitely extended plane front, we write formulas for the correlation of the main values that characterize vibrations in this wave:

$$v = jk\varphi; \quad p = j\omega\rho\varphi; \quad u = -\varphi/c; \quad p = \rho cv. \quad (2.12)$$

In the practice of acoustic testing that includes the AE testing methods, the wave processes limited in time and space are used. Instead of monochromatic vibrations, pulses are most often applied. A pulse (from “*impulses*” in Latin = “impact” or “push”) is the time-limited vibration process. The amplitude of vibrations in a pulse changes from zero to the final value according to the law that describes the pulse shape [4]. The time during which the amplitude exceeds 0.1 of its maximum value is considered to be the pulse duration τ . The product $c\tau$ is called a spatial duration of a pulse. It determines a space region occupied by a pulse. Using the formulas of spectral analysis, the pulse is represented as a frequency integral of monochromatic vibrations of a different frequency, i.e., it is expanded in the harmonic vibrations spectrum.

No success was achieved in obtaining a limited wave in the form of a bundle of parallel rays. For example, by cutting out a part of the plane wave front by a diaphragm, a complicated wave field is obtained. In practice, however, the weakly scattered ray bundles are used. A wave with an arbitrary front can be represented as an assembly of plane waves by decomposing in the Fourier integral over a wave vector k . For a durable enough acoustic pulse that propagates in a direction of the weakly scattered ray bundle, formulas (2.12) are used, although in this case, as approximate ones [1].

The Laplace operator ∇^2 in Eq. (2.8) can be represented not only in Cartesian but also in cylindrical or spherical coordinates. Accordingly, the simplest solutions of Eq. (2.8) will have the form not of a plane but of cylindrical or spherical waves. A harmonic spherical wave that starts from the origin of coordinates looks like

$$\varphi = \frac{\Phi}{r} e^{j(\mathbf{k}\mathbf{r} - \omega t)}. \quad (2.13)$$

Here, \mathbf{r} is the radius vector that radiates from the origin of coordinates, and the direction of \mathbf{k} coincides with \mathbf{r} , $k_x = k_y = k_z$. A surface with a constant phase, i.e., the wave front, has the form of a sphere for this wave, and the rays radiate in the direction of the radii. The wave amplitude decreases inversely proportional to the distance along a ray. At large distances r , an insignificant part of a spherical wave front can be considered to be a quasi-plane wave.

In the case of a sphere-like emitter of radius a that pulsates by volume changing with constant frequency and amplitude of vibration velocity, the pressure in an outgoing spherical wave is written as [5]:

$$p = \frac{ja^2|v_0|\rho\omega}{r} e^{j(\mathbf{k}\mathbf{r} - \omega t)} \approx j \frac{|p_0|}{\lambda r} 2\pi a^2 e^{j(\mathbf{k}\mathbf{r} - \omega t)} \quad (2.14)$$

where p_0 is the pressure near the sphere, calculated approximately by formula (2.12).

Elastic wave energy consists of the kinetic energy of medium particles motion and internal (potential) energy of deformation. The density of the kinetic energy is equal to $\rho|\mathbf{v}|^2/2$ [1]. In a running wave, the internal energy density is equal to the density of the kinetic energy, so the total energy density is $E = \rho|\mathbf{v}|^2$. The density of the energy flux is

$$W = cE = \rho c|\mathbf{v}|^2 = |p\mathbf{v}| = |p|^2 / \rho c. \quad (2.15)$$

The time average value of the energy flux density is called the elastic wave intensity. For a plane harmonic running wave, the intensity is determined as

$$J = |p|^2 / 2\rho c = \rho c|\mathbf{v}|^2 / 2. \quad (2.16)$$

In a spherical wave, the intensity decreases inversely proportional to the distance squared:

$$J = |p_0|^2 2\pi^2 a^4 / (\lambda^2 \rho c r^2). \quad (2.17)$$

Acoustic waves attenuate when passing in the real media, and this is not accounted for by Eqs. (2.6) and (2.7). As a result, a wave number becomes a complex one: $k = k' + j\delta$, where δ is the attenuation factor. A plane wave that propagates along the x axis with the account of attenuation is written as

$$\varphi = \Phi e^{-\delta x} e^{j(k'x - \omega t)}. \quad (2.18)$$

2.1.4 Spatial Elastic Waves

By using Eq. (2.5) or (2.6), it is possible to show that in the infinite solid medium there are two types of waves that propagate with different velocities [3]. It is known from the vector analysis that any vector field can be represented as a sum of two vectors, one of which has a scalar potential and the other a vector one:

$$\mathbf{u} = \mathbf{u}_l + \mathbf{u}_t = \text{grad}\varphi + \text{rot}\boldsymbol{\psi}. \quad (2.19)$$

Taking into consideration that $\text{rot } \mathbf{u}_l = \text{div } \mathbf{u}_t = 0$ and substituting (2.19) into (2.6) with the application of operations rot and div , we get

$$\partial^2 \mathbf{u}_l / \partial t^2 - c_l^2 \nabla^2 \mathbf{u}_l = 0; \quad c_l = \sqrt{(\Lambda + 2\mu)/\rho}, \quad (2.20)$$

and

$$\partial^2 \mathbf{u}_t / \partial t^2 - c_t^2 \nabla^2 \mathbf{u}_t = 0; \quad c_t = \sqrt{\mu/\rho}. \quad (2.21)$$

Equations (2.20) and (2.21) are of the wave type and are similar to Eq. (2.7). Hence, the vector \mathbf{u} in a solid decomposes into two waves propagating with different velocities.

The wave \mathbf{u}_l is called a longitudinal wave or a wave of expansion-compression (Fig. 2.1), because the vibration direction in it coincides with its propagation direction. For the volume strain ε , the same Eq. (2.20) is satisfied.

The wave \mathbf{u}_t in which the direction of vibrations is perpendicular to the direction of wave propagation and in which deformations are shear is called a transversal or shear wave (Fig. 2.2). There are no transversal waves in liquids and gases due to the absence of shape elasticity in these media. Strictly speaking, in liquids, there are waves similar to transversal ones, in which vibrations are transferred due to ductile forces; however, they decay quickly [1]. The ratio of velocities of longitudinal and transversal waves depends on the Poisson's ratio ν of the medium. For example, in metals, where $\nu \approx 0.3$, it is possible to get $c_l/c_t \approx 0.55$ (see Table 2.1).

When a transversal wave propagates in an infinite isotropic medium, all directions of transversal vibrations are equal. If there is a limiting surface, to which a transversal wave propagates parallel or at an angle, the question arises regarding the direction of vibrations in the transversal wave with respect to this surface. The wave, in which the direction of vibrations is parallel to the limiting surface, is called "horizontally polarized" (TH-wave). If vibrations occur in the plane perpendicular to the separating surface, such a wave is called "vertically polarized" (TV-wave). This type of wave is more frequently used in non-destructive testing. Therefore, if no special notations are given, by transversal wave we mean a vertical polarized wave [1].

In ultrasonic testing, a longitudinal wave is usually excited by special piezo-electric transducers that cause tension: compression deformation at a certain part of

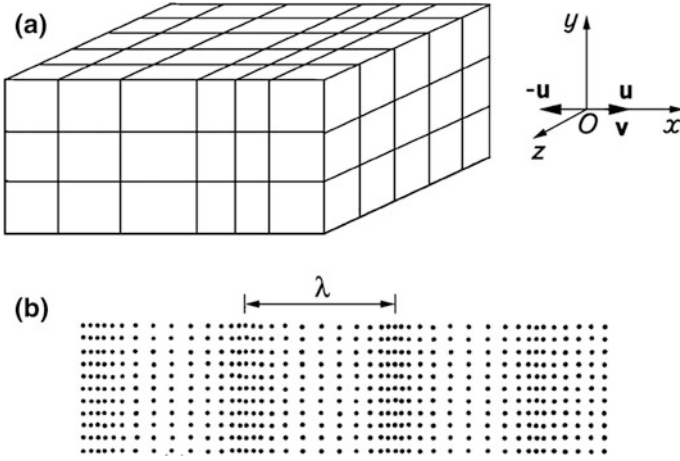


Fig. 2.1 Propagation of longitudinal wave vibrations (schematically)

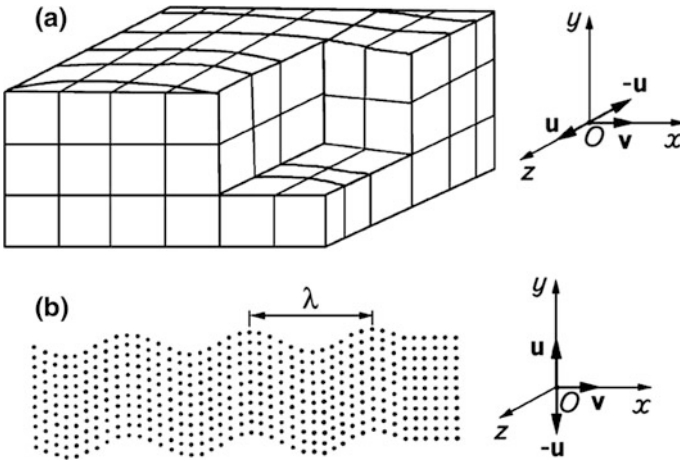


Fig. 2.2 Distribution of transversal wave vibrations (schematically): **a** is TH-wave; **b** is TV-wave

the IO surface, and a transversal wave—by shear deformation. Most often, a vertical polarized wave inclined to the surface is excited by a longitudinal incident wave at a certain angle to the IO surface from an external medium. Thus, the incident longitudinal wave is transformed into a transversal one. The external medium, from which a longitudinal wave falls at a certain angle, is called a “prism of a transducer” [6].

Table 2.1 Elastic properties of some media [1]

Material	Density ρ , 10 ³ kg/m ³	Velocity of wave propagation c , 10 ³ m/s			Wave resistance for longitudinal waves, z , 10 ⁶ Pa × s/m
		Longitudinal	Transversal	Surface	
<i>Metals</i>					
Aluminum	2.7	6.35	3.08	2.80	17.1
Beryllium	1.82	12.8	8.71	7.87	23.3
Bronze	8.5...8.9	3.5...3.8	2.3...2.5	2.1... 2.3	31...33
Bismuth	9.80	2.18	1.10	1.03	21.4
Tungsten	19.3	5.18	2.87	2.65	100
Duralumin	2.7...2.8	6.25...6.35	3.1	2.9	17.2...17.5
Iron	7.8	5.91	3.23	3.0	46.1
Gold	19.3	3.24	1.20	1.12	62.5
Cadmium	8.6	2.78	1.5	1.4	27.0
Brass composition-metal	8.5	4.43	2.12	1.95	37.7
Lithium	0.53	3.00	–	–	1.6
Magnesium	1.74	5.77	3.05	2.875	10.1
Copper	8.9	4.72	3.72	3.52	42.0
Molybdenum	10.1	6.29	3.35	3.11	63.5
Nickel	8.8	5.63	2.96	2.64	49.5
Niobium	3.9	4.10	1.70	1.58	35.3
Tin	7.3	3.32	1.67	1.56	24.2
Platinum	21.4	3.96	1.67	1.57	84.6
Mercury	13.6	1.45	–	–	19.8
Lead	11.4	2.16	.0.70	0.63	24.6
Silver	10.5	3.60	1.59	1.48	38.0
Steel corrosion-resistant	8.03	5.73	3.12	2.90	46.6
Carbon steel	7.80	5.92	3.28	3.01	46.1
Titan	4.50	6.00	3.50	3.20	27.0
Uranium	18.7	3.37	1.94	1.8	63.0
Zinc	7.1	4.17	2.41	2.22	29.6
Zirconium	6.5	4.65	2.25	2.15	30.2
Cast-iron	7.2	3.5...5.6	2.2...3.2	–	25...40
<i>Non-metals</i>					
Araldite	1.18	2.5	1.1	–	3.0
Capron	1.1	2.64	–	–	2.9
Quartz melted	2.2	5.93	3.75	3.39	13.0
Nylon, perlon	1.1...1.2	1.8...2.2	–	–	1.8...2.7

(continued)

Table 2.1 (continued)

Plexiglass	1.18	2.65...2.73	1.12...1.13	1.05	3.0...3.22
Aluminum oxide	3.7...3.9	10	–	–	37...39
Polystyrene	1.1	2.37	1.12	1.04	2.61
<i>Rubber</i>					
Raw	1.3...2.1	1.5	–	–	1.9...3.1
Vulcanized	0.9...1.6	1.5...2.3	–	–	1.3...3.7
Resin acrylic	1.18	2.6	1.12	–	3.2
Window glass	2.6	5.7	3.4	3.1	14.5
Textolite	1.2...1.3	2.6	–	–	3.1...3.9
Fluoroplastic	2.2	1.35	–	–	3.0
Porcelain	2.4	5.3...5.35	3.5...3.7	–	12.8
Ebonite	1.2	2.40	–	–	2.9
Epoxy resin hard	1.15...1.3	2.5...2.8	1.1	–	2.8...3.7
<i>Liquids (20 °C)</i>					
Acetone	0.792	1.192	–	–	0.4
Water	0.998	1.90	–	–	1.49
Glycerin	1.265	1.923	–	–	2.42
Kerosene	0.825	1.295	–	–	1.07
Acetic acid	1.05	1.84	–	–	1.45
<i>Oil</i>					
Diesel	0.88...1.02	1.25	–	–	1.1...1.3
Machine	0.89...0.96	1.74	–	–	1.5...1.7
Transformer	0.9...0.92	1.38...1.40	–	–	1.25...1.27
<i>Alcohol</i>					
Methyl	0.792	1.123	–	–	0.89
Ethyl	0.789	1.180	–	–	0.93
<i>Gases (0 °C)</i>					
Hydrogen	0.9×10^{-4}	1.248	–	–	1.1×10^{-4}
Air	1.3×10^{-3}	0.331	–	–	4.3×10^{-4}

2.1.5 Rayleigh Surface Wave

A specific type of waves propagate along the solid surface. For an unloaded (free) surface, the existence of some of them is proved in the following way [6]: We can assume a priori that there is a wave running along the solid boundary (along the x axis) and it consists of a linear combination of longitudinal and transversal vibrations, the amplitudes of which depend on the depth y under the surface (Fig. 2.3). For this purpose, the velocities of propagation of transversal vibrations should be the same and equal to some value c_s , while the wave number should be

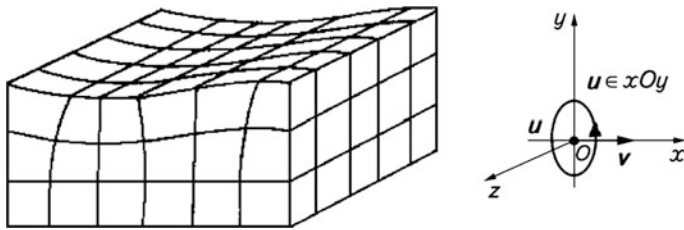


Fig. 2.3 Schematic presentation of the Rayleigh wave propagation on the free surface of a solid

equal to $k_s = \omega/c_s$. These predicted solutions are substituted into wave equations (2.20) and (2.21), which satisfy the conditions:

$$u_t = A \exp\left(-\sqrt{k_s^2 - k_t^2}y\right) \exp(-jk_s x),$$

and

$$u_l = B \exp\left(-\sqrt{k_s^2 - k_t^2}y\right) \exp(-jk_s x). \quad (2.22)$$

Here, and further, a multiplier $e^{-j\omega t}$ is omitted. Thus, the obtained expressions correspond to the class of heterogeneous waves. In this wave, the amplitude changes in the front direction (along the y axis).

Functions (2.22) are to be substituted in boundary conditions of the equation: normal and tangential stress components vanish on a free surface, i.e., $\sigma_{yy} = 0$, $\sigma_{xy} = 0$. Two unknowns k_s/k_t and a ratio A/B of amplitudes are found from these two equations. For $(k_s/k_t)^2$, the 3rd degree equation is obtained. One real and positive root proves that an a priori assumption is correct and that the wave that was sought really exists.

An approximate formula for evaluating the velocity of the Rayleigh surface wave is known [1]:

$$c_s \approx c_t(0.87 + 1.12\nu)(1 + \nu)^{-1} \approx 0.93c_t \quad (2.23)$$

for condition $\nu = 0.3$. The absence of the imaginary part in a root for k_s indicates a weak decay of the surface wave caused just by an ordinary spatial wave decay, which is why the Rayleigh wave can propagate over a large distance along the solid surface. Its penetration underneath the surface of the body is small: at the wavelength λ_s , the intensity is about 5% of the intensity on the surface of the body.

During the surface wave propagation, the body particles move, revolving around ellipses (Fig. 2.3) with a large axis perpendicular to the surface forming a TV-type wave, and the extension of the ellipse increases with the depth. These conclusions yield from formulas (2.22), in which the greater the decrease of multipliers with depth, the greater the difference $k_s^2 - k_{l,t}^2$. A wave similar to the Rayleigh wave,

i.e., a quasi-Rayleigh wave, can propagate not only along a plane but also along a distorted surface. On concave areas of the surface, the wave undergoes further damping. The greater the damping, the smaller the curvature radius due to the energy irradiation into the body depth. Therefore, the velocity of the Rayleigh wave decreases on concave areas, while on convex areas it increases. The wave selectively responds to the defects, depending on the depth of their location. The defects on the surface produce a maximum reflection, while at the depth that is greater than the wavelength, they are practically undetected.

2.1.6 Head (Creeping) Wave

When analyzing the solution to the problem on excitation of elastic waves upon a certain area of a solid surface, we can see that a wave propagates along the surface with the velocity practically equal to the velocity of a longitudinal wave. In [3, 6] it is referred to as a quasi-homogeneous wave because the amplitude along its front changes slowly. However, in the literature, such a wave is usually called a “head” or “creeping wave.”

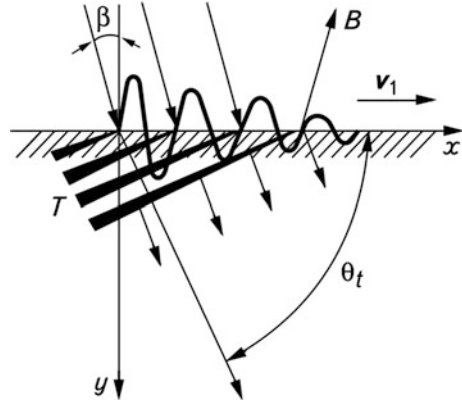
At every point on the surface along which a head wave propagates, a transversal wave is excited at an angle θ_t to the surface which is determined as $\theta_t = \arcsin(c_t / c_l)$. As a result, the head wave decays rapidly. Such waves, with a velocity smaller than that of a generating wave, are called “side waves.” The combination of a head wave and side wave provides the situation with the stresses being equal to zero on the free surface of the body. Waves that consist of surface and spatial components, in which a surface component is continuously transformed into a spatial one, belong to the type of leaky waves [1, 6].

The head wave is usually excited by a longitudinal wave that falls inclined from the external medium (a prism) onto a partial area of the IO surface at an angle $\beta = \arcsin(c_0 / c_l)$ (Fig. 2.4). The bundle of longitudinal waves radiates from this area of the surface, with one of the rays passing along the surface—this ray actually being the head wave. The ray that propagates at an angle of $10 \dots 15^\circ$ to the surface has the maximum energy of irradiation. The fronts of transversal waves T , generated by the head wave, are shown by lines whose width expands with an increase of the depth that corresponds to the wave amplitude increase. This takes place due to an increase of the number of surface points, which contribute to the formation of a side transversal wave.

Concurrent with the excitation of waves in IO, the waves in a prism are also excited. In seismic acoustics, a side wave is called a “ B wave,” which corresponds to a side wave in a prism. In seismic acoustics, it is referred to as a “head wave.”

A quasi-homogeneous (head) wave is almost insensitive to surface defects and to a surface roughness. Nevertheless, it can be used for locating surface defects in a layer, beginning with the depth of $1 \dots 2$ mm. by these waves. It is difficult to test thin structures by the side transversal waves that reflect from the opposite surface of IO and give off false signals [1].

Fig. 2.4 Propagation of a head (creeping) wave on the free surface of a solid (schematically) [6]



2.1.7 Waves at an Interface of Two Media

The waves on the free surface of a solid are discussed above. An external medium on a limited area of the surface was introduced just to explain the wave excitation mechanism. When the solid surface is loaded with a liquid or hard medium, specific types of waves appear [1, 3, 6–8].

For a solid-liquid interface, with the sound velocity in a liquid $c_p < c_s$, a surface wave along the interface generates a side wave in a liquid and thus decays (Fig. 2.5a). For a steel-water interface, a side wave amplitude decreases e times at a distance of $10 \lambda_s$. This feature classifies the wave as a leaking one.

Moreover, a wave can predominantly propagate in a liquid with a velocity less than c_p (Fig. 2.5b). In a solid, it is located in a layer of a thickness $\lambda_p/2\pi$, while in a liquid it is located in the layer of a thickness much larger than λ . The wave is used for testing the solid material surface by an immersion method. Similarly to the Rayleigh wave, it decays very slowly with the distance along the surface.

For an interface of two solid media (Fig. 2.5c) whose elastic modules and density differ insignificantly, the Stoneley wave propagates along the interface. It consists of something like two Rayleigh waves, each existing in its own medium, but both with identical propagation velocities that are lower than the velocities of spatial waves in both media. In each medium, the wave is localized in a layer of the thickness of a wavelength order and is vertically polarized. Such waves are used for the inspection of bi-metal joints.

Transversal waves propagating along the interface of two media and being horizontally polarized are referred to as the “Love waves” (Fig. 2.6). They arise when there is a layer of solid material on the solid half-space surface, with the velocity of transversal waves propagation less than in a half-space. The depth of the wave penetration in a half-space increases with a decrease of the layer thickness. When there is no layer, the Love wave in a half-space transforms into a spatial one, i.e., into a horizontally polarized plane transversal wave. The Love waves are used for testing the quality of coatings on the IO surface.

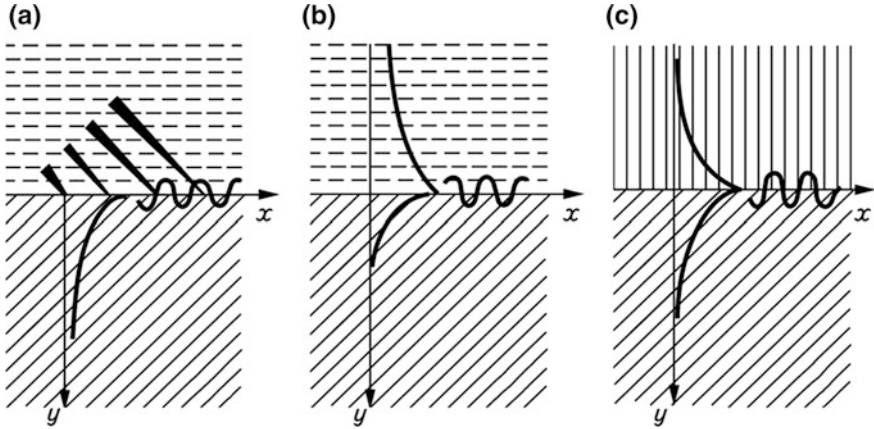


Fig. 2.5 Types of waves at the interface of two media: **a** is the decaying Rayleigh wave at the solid-liquid interface; **b** is the weak decaying wave at this interface; **c** is the Stoneley wave at the two solids interface

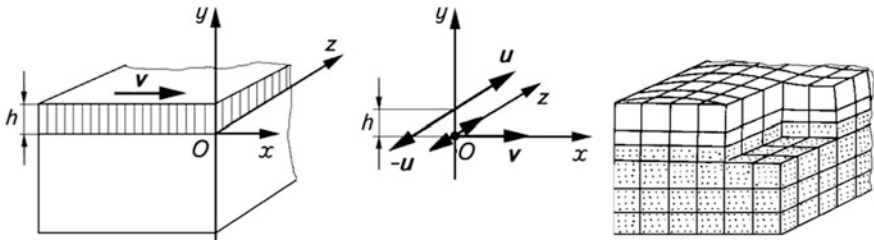


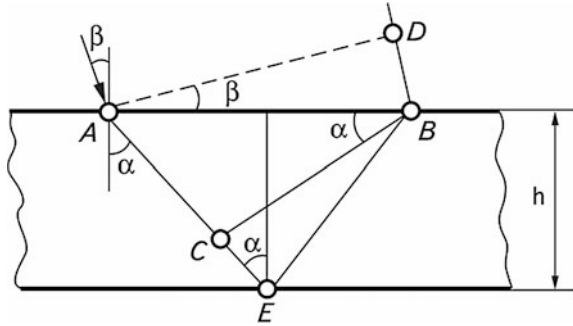
Fig. 2.6 Schematic representation of the Love wave propagation in a layer—half-space system

2.1.8 Waves in Layers and Plates

In bodies containing two free surfaces (a plate), specific types of elastic waves can propagate [1, 3, 6, 7]. They are called the “waves in plates” or the “Lamb waves” and are attributed to the normal waves, namely the waves propagating (transporting the energy) along a plate, a layer or a bar, and stationary waves (where energy is not transported) in a perpendicular direction. The solution to the wave equation for a plate with boundary conditions, when stresses on both surfaces are equal to zero, gives a system of two characteristic equations for the wave number k_p . It has two or more positive real roots, depending on the product of a plate thickness and frequency. A certain type of the wave (a mode) in the plate corresponds to each root.

To illustrate the physical essence of the waves in plates, let us consider the formation of normal waves in a liquid layer. Let a plane longitudinal wave fall outside onto a layer of thickness h (Fig. 2.7) at an angle β . Line AD shows the incident wave front. Because of the refraction at the interface, the wave with a CB

Fig. 2.7 Formation (schematically) of normal waves in a layer of liquid



front arises in the layer. The wave propagates at an angle α and reflects many times in the layer. At a certain angle of incidence, the wave reflected from the lower surface coincides in a phase with a direct wave that propagates from the upper surface. We can define the angles β or α , $\sin \beta / c_1 = \sin \alpha / c_2$, where c_1 and c_2 are velocities of the sound in a media, at which this phenomenon is observed.

As is known, the difference phases of the direct and the reflected waves are determined as

$$2\pi \left(\frac{AEB}{\lambda_2} - \frac{DB}{\lambda_1} \right) = 2\pi \left(\frac{2h}{\lambda_2 \cos \alpha} - \frac{2h \operatorname{tg} \alpha \sin \alpha}{\lambda_1} \right) = \varphi. \quad (2.24)$$

Here, λ_1 and λ_2 are the wavelengths in an upper medium and in a layer. The condition of phase coincidence is attained if $\varphi = 2n\pi$, where n is an integer. Hence,

$$h \cos \alpha = n \lambda_2 / 2. \quad (2.25)$$

Thus, a wave in a layer is caused by the interference of the waves propagating in different directions. Interference (from the Latin “*inter*,” meaning “mutually,” and “*ferio*” meaning to “strike” or “hit”) is the process of combining two or several waves in space. A monochromatic wave that spreads zigzag-like along a layer under condition (2.25) can be considered to be a wave that envelopes all the sections of a layer and moves along it. It differs from the above-mentioned waves by the velocity that varies, depending on frequency, i.e., velocity dispersion takes place.

Using a wave in a layer as an example, it is convenient to consider the concept of phase and group velocities. A group velocity characterizes the velocity of energy propagation in the direction of a wave motion. A wave pulse is a typical energy carrier. Since a pulse in a layer propagates zigzag-like, the energy propagation velocity by this wave along a layer is (Fig. 2.8) [1]:

$$c_g = c_2 \sin \alpha. \quad (2.26)$$

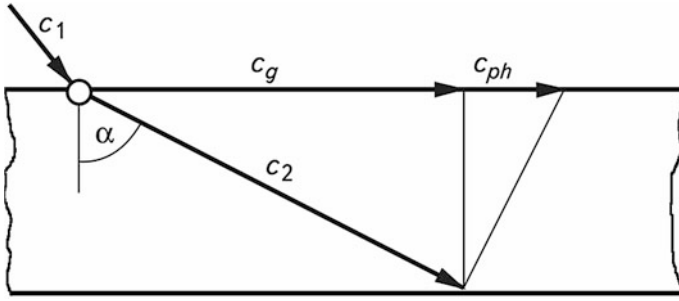


Fig. 2.8 Relationship between spatial c_2 , group c_g and phase c_{ph} velocities of waves in a medium

A phase velocity determines the velocity of phase propagation in the direction of wave propagation. It is equal to the velocity of the phase variation of an incident wave along the layer, i.e., it is determined from the sine law:

$$\sin\beta/c_1 = \sin\alpha/c_2 = 1/c_{ph}; \quad c_{ph} = c_2/\sin\alpha. \quad (2.27)$$

Since a newly formed wave moves along the layer, its refraction angle is 90° . The angle α is evaluated from (2.25). As a result, we get

$$c_g = c_2 \sqrt{1 - (n\lambda_2/2h)^2}; \quad c_{ph} = c_2 / \sqrt{1 - (n\lambda_2/2h)^2}. \quad (2.28)$$

Thus, the phase and group velocities of normal waves depend on the frequency of elastic vibrations and the layer thickness. The dispersion curves, i.e., the graphs of the c_{ph}/c_2 versus h/λ_2 dependence are shown in Fig. 2.9. At the points where $h/\lambda_2 = 1/2; 1; 3/2$, etc., phase velocities tend to infinity. It means that the whole surface vibrates simultaneously, and c_g in these cases is equal to zero.

When $h/\lambda_2 \rightarrow \infty$, for all values of n , velocities c_g and c_{ph} of normal waves tend to c_2 , i.e., the spatial wave velocity. The waves with the odd values of n are called symmetric because the motion of particles within these waves is symmetric about the layer axis, and the waves with even values of n are antisymmetric.

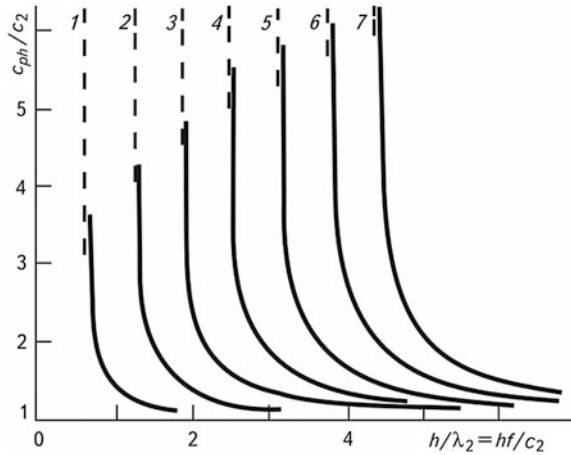
The formula for the relation of phase and group velocities is known

$$\frac{1}{c_g} - \frac{1}{c_{ph}} = -\frac{f}{c_{ph}^2} \frac{dc_{ph}}{df}. \quad (2.29)$$

Dependences (2.27) and (2.28) satisfy this equation.

Regarding solid layers (plates), it should be noted that the essence of the phenomenon, i.e., the formation of standing waves along a plate thickness due to interference of normal waves, remains here, although the conditions of formation of normal waves are more complicated due to the presence of longitudinal and transversal waves. Due to reflection, these waves are partly transformed into one another, and the wave phase can vary by an aliquant π number.

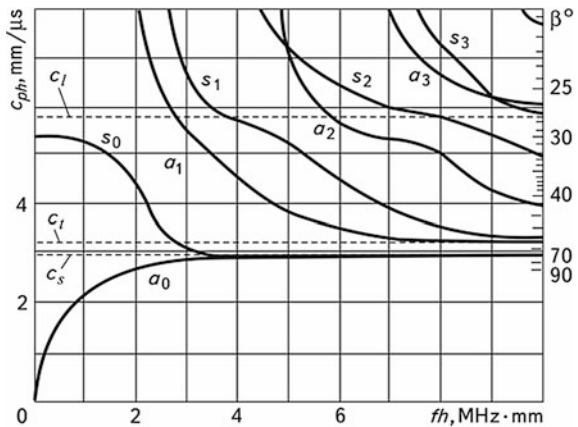
Fig. 2.9 Dispersion curves of normal waves propagating in a liquid layer



In Fig. 2.10, a system of dispersion curves for the phase velocity of waves in a steel plate is plotted. Zero indices indicate the modes that transform into a surface wave with an increase of the plate thickness. These waves exist at any frequency and for any thickness of plates. A zero symmetric mode s_0 (Fig. 2.11a) corresponds to the wave of extension-compression, while a zero antisymmetric mode a_0 under condition $h \ll \lambda$ (Fig. 2.11b) corresponds to the bending wave. For a wave s_0 under condition $fh \rightarrow 0$, phase and group velocities are the same since there is no dispersion.

In the considered modes of normal waves, the medium particles vibrate in their propagation plane. They are caused by the interference of longitudinal and transversal vertical polarized waves. In a plate, the waves can also be formed due to the interference of transversal horizontally polarized waves. When the waves are reflected from the plate boundaries, the waves with horizontal polarization are not

Fig. 2.10 Dispersion curves of the Lamb waves in a steel plate: c_l , c_t and c_s are the velocities of longitudinal, transversal and surface waves; a_0, a_1, a_2, \dots are antisymmetric modes; s_0, s_1, s_2, \dots are symmetric modes of vibrations



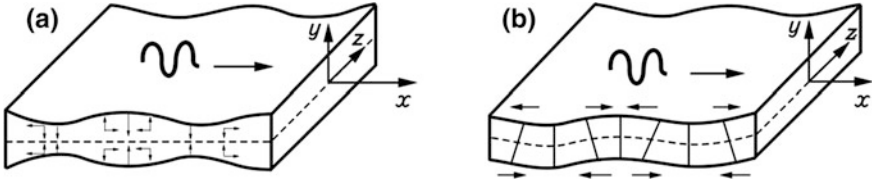


Fig. 2.11 Schematic representation of normal symmetric (a) and antisymmetric (b) waves: x is wave propagation direction (arrows indicate directions of displacements along the x and y axes)

subjected to transformation, and a system of dispersion curves is similar to that shown in Fig. 2.9.

In a plate, as well as in a waveguide, normal waves propagate over large distances. This permits using them successfully in testing the sheets, shells, and pipes that are 3...5 mm or less thick. The change of the waveguide cross-section and the presence of heterogeneity (defects) in it, cause the reflection of normal waves. It should be noted that the changes in the wave propagation conditions in a waveguide are caused not only by transversal but also by longitudinal defects—for example by the laminations located along the wave propagation direction. The defects located along the spatial wave propagation direction are poorly detected; this feature is useful in flaw detection.

As has already been shown above, the Love waves are very important surface waves that propagate in a layered media. The phase velocity of a Love wave is higher than the velocity of a transversal wave in a layer, although it is lower than their velocity in a half-space. From the solution of the known equations [7], it follows that the dispersion of Love waves is due to the presence of a dimensional parameter, i.e., a layer thickness.

Strictly speaking, Love waves are not true surface waves because they are caused by layered media. Various roots of a dispersion equation characterize the corresponding normal modes, and their number is larger than the product of the wave number k_2 (transversal wave) and the layer thickness h . Sometimes, Love waves are interpreted simply as the lower mode of vibrations that exists on all layer thicknesses, including the condition $k_2 h \rightarrow 0$. These waves, like the Rayleigh waves, are observed during earthquakes, since the earth's crust has a lamellar structure. Lately, they have been used for the creation of dispersion delay lines.

2.1.9 Waves in Bars

In bars, as well as in plates, there are normal waves that propagate in the direction of their length and create a system of standing waves in a transversal cross-section. These waves are sometimes called the Pochhammer waves. For bars with a different shape of the cross-section (round, square and other), special systems of dispersion

curves take place that indicate symmetric and asymmetric modes. The velocity of a mode s_0 in a bar is less than in a plate.

Except for the already mentioned symmetric and asymmetrical waves, a twist wave can propagate in a bar or a pipe. Vibrations in a twist wave arise due to rotation about an axis of a certain cross-section of a bar or a pipe. Different modes of normal waves in a bar are excited by an off-normal incidence of a longitudinal wave from an external medium or by electromagnetic-acoustic method (a twist wave).

2.1.10 Other Types of Waves

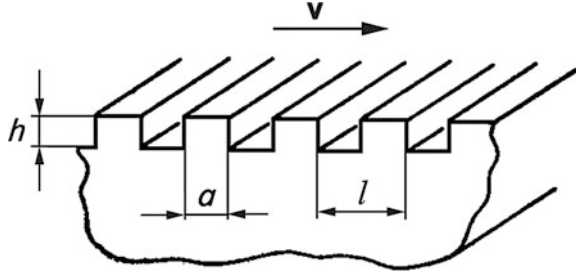
Besides the waves described above, there are other types of surface waves in solids that can be used in technical diagnostics and nondestructive testing of objects. First of all, the surface waves in crystals must be mentioned [3, 5, 7]. Today, the existence of surface waves in most directions of any cross-section of crystals is proved. Owing to the anisotropy of their elastic properties, a plane surface wave has three components of displacement, and its wave vector does not coincide with the direction of the group velocity vector. Only for crystal symmetric directions, the vectors of the group and phase velocities are collinear, and the paths of particles lie in the plane that passes through the wave vector and a normal to the surface. These surface waves are very similar to the Rayleigh waves in an isotropic solid, and so they are sometimes called the “Rayleigh-type waves” [5].

A typical example of such a wave is the wave that propagates in the ZY direction—the cross-section of the lithium niobates piezoelectric crystal. It is worth noting that in piezo-crystals, the surface wave is usually accompanied by a quasi-static electric field, and this feature is used in different acoustic-electronic devices of signal processing.

A piezoelectric effect in a number of cases leads to the formation of purely shear surface waves known in the literature as the “Guliaev-Bleustein” waves. They, unlike the Rayleigh waves, are weakly heterogeneous and decrease with depth at a certain distance depending on the coefficient of electromechanical coupling. Hence, they depend less on the surface irregularities and are used in the acoustic-electric devices that operate at super-high frequencies. The waves of this type can exist in non-piezoelectric materials at the presence of external fields: electric (due to a resulting piezoelectric effect), and magnetic (the action of the Lorentz force on electrons in metals). In such cases, it is possible to inspect the depth of the wave localization by applying a field of specific value [7].

There is an analogy, however, only with the electromagnetic waves in a metallic comb, for shear surface waves that propagate along a periodically unequal solid boundary (Fig. 2.12) [7]. Wave equations and critical conditions in both cases are identical. Therefore, it is possible to reach the conclusion, based on the known solution for electromagnetic waves, that in the system under discussion a surface wave can propagate with the phase velocity of

Fig. 2.12 A comb-like structure on a solid surface



$$c = c_t \left[1 + (a/l)^2 \operatorname{tg}^2(kh) \right]^{-1/2}, \quad (2.30)$$

where a , l and h are the geometrical parameters of a medium of propagation of waves, k is the wave number.

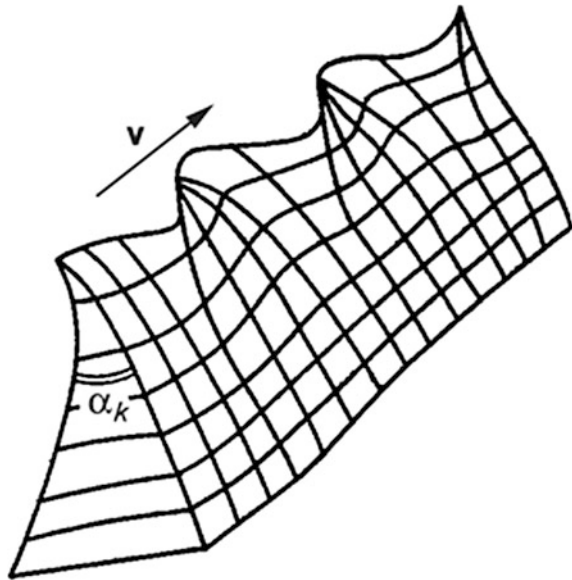
Equation (2.30) is valid under condition $kl \ll 1$. Thus, it yields that at certain values of a , l , and h , the surface wave velocity c can be significantly less than c_t .

A number of surface waves are defined purely by geometrical factors. On a convex cylinder surface of a solid, except for the Rayleigh type waves, there should also be non-Rayleigh surface waves with polarization in the plane that passes through a wave vector and a normal to the surface. A component of longitudinal motion in those waves behaves like the motion in the Rayleigh wave, decreasing with depth by an exponential dependence. A shear component, decaying with depth, oscillates; such waves are called “mixed-type” waves. Their velocity is somewhat higher than the velocity of a shear wave, and it is attained asymptotically with an increase of the cylinder radius. In convex cylinders, there are purely shear surface waves that are polarized parallel to the surface. Since the reflection of horizontally polarized shear waves is similar to the reflection of waves in a liquid, such surface waves do not differ from mixed-type ones.

Other linear waves, which propagate along the elastic wedge edges, are also known to exist (Fig. 2.13) [7]. They represent another class of wave motions of a continuum that concentrates near the surface borders. The waves are similar to the surface ones, but they have not been studied comprehensively. They are analyzed by numerical methods, and calculations illustrate that an arbitrary field at the wedge edge, similar to any other waveguide, can be represented as the sum of vibration modes that propagate along the edge with their inherent phase velocities.

From the practical viewpoint, the most important modes of a wedge are the lower anti-symmetric ones. Their amplitudes also quickly decrease with depth, so that practically all the energy of a wave remains concentrated near the edge line. Owing to this fact, such waves are called linear or wedge waves. They are not dispersion waves, because the wedge is characterized only by an opening angle α_k rather than by linear sizes. The velocity of wedge waves diminishes with a decrease

Fig. 2.13 Anti-symmetric vibrations of the wedge edge (schematically)



of α_k and can be less than the velocity of a spatial transversal wave if $\alpha_k \approx 5 \dots 10^\circ$ by one order of magnitude. Physically this is clear, because anti-symmetric waves in a sharp wedge are similar to those in a thin plate. The latter ones are also called the “lower anti-symmetric Lamb” modes or “bend waves.”

Finally, we should mention Sesave waves and the waves caused by the mechanisms of the field non-locality that are related to the medium microstructure. The first ones arise in the system: layer half-space, similar to the Love waves under condition of a small thickness of a layer (Fig. 2.6). In this case, there is only one mode of vibration, which transforms into a Rayleigh wave when $kh \rightarrow 0$. The following mode of such vibrations is a “Sesave” wave. It occurs when the velocity of transversal waves in a layer is larger than the transversal velocity of a sound in a half-space. These waves, as well as the Lamb waves, are widely used in acoustic electronics for making the surface wave waveguides operate according to a general principle of open waveguides [6].

The second ones cannot be explained from the position of continuum mechanics. The use of non-local continuum models permits predicting the occurrence of strongly heterogeneous surface waves whose amplitude also decreases at the depth of the order of atomic spacing in a lattice.

The surface wave types in solids discussed in this chapter do not include all the types of waves occurring in nature. This concerns, first of all, the waves in layered media [3, 4] and the others caused by various mechanisms.

2.2 Some Basic Acoustic Properties of Media

Acoustic properties of a medium are determined by its physico-mechanical properties: density, elasticity, structure, etc. The velocity of acoustic waves propagation for liquids or gases is determined at a given state of the medium (temperature, pressure) by a constant $c = \sqrt{(\partial p / \partial \rho)_s} = \sqrt{K\rho}$, where p is the pressure in the medium, and K is the module of a uniform compression (the ratio of pressure to the strain of volume change with a reverse sign). The index s shows that the derivation is done at a constant entropy. The velocity, as a rule, does not depend on frequency. However, in some materials the dispersion of velocity is observed in a certain frequency range, i.e., the dependence of velocity on the number of degrees of freedom of vibration motion of a molecule. In the frequency range that has been mentioned, an additional degree of freedom should be involved in vibrations: mutual motion of atoms inside the molecule. Investigation of the properties of materials and the kinetics of molecular processes by measuring velocity and damping of acoustic waves is the subject of molecular acoustics. Isotropic solids are characterized by the velocities of elastic wave propagation determined by formulas (2.20) and (2.21) (see Table 2.1). These two values of velocities can be used as a pair of elastic constants instead of the Lamé coefficients or modules of elasticity.

A crystal solid is an anisotropic medium. Its properties vary depending on the directions, and the maximum possible number of independent elastic constants is 21. However, the presence of a crystal symmetry diminishes the number of independent elastic constants for the majority of them. In a crystal, three elastic waves can propagate with different velocities in every direction. In an isotropic solid, longitudinal wave and two transversal waves with mutually perpendicular directions of vibrations correspond to them. The velocities of these transversal waves are identical. In a crystal, a displacement vector in each wave has the components, which are both parallel and perpendicular to the propagation direction, i.e., each wave will be neither purely longitudinal nor purely transversal [1].

The group velocity that determines the direction of the energy flow \mathbf{J} , due to the anisotropy of crystal characteristics, does not coincide with the direction of the wave vector \mathbf{k} , although the wave fronts remain perpendicular to \mathbf{k} . An angle between \mathbf{J} and \mathbf{k} is spatial and can be of tens of degrees.

The acoustic wave propagation velocity is a function of temperature. This dependence is characterized by a change of velocity by one degree of temperature. For gases, this value is positive, while for liquids and solids, it is negative—an order of 0.01...0.05%.

2.2.1 Impedance and Wave Resistance of a Medium

The term “impedance” (from the Latin “*impedio*,” meaning “oppose”) means “resistance.” Acoustic impedance is determined as a ratio of a complex sound pressure

to a spatial vibration velocity. This concept is used, in particular, for the description of acoustic wave propagation. In the extended medium, the concept of specific acoustic impedance is introduced by using the correlation of sound pressure with the vibration velocity (not spatial). Since only this case is considered here, the term “specific” is omitted (a mechanical impedance differs from an acoustic) in what follows.

If a plane harmonic wave propagates in a liquid medium, then according to formula (2.12), acoustic impedance is equal to $z = p/v = \rho c$. This value characterizes a medium in which the wave propagates. It is called the “wave resistance” of a medium or its characteristic impedance. This concept of impedance is also used for a solid (for longitudinal and transversal waves), defining it as a ratio of the corresponding mechanical stress to the vibration velocity of a medium particles taken with a reverse sign (see Table 2.1).

The origin of the term “impedance” is related to the system of electromechanical analogies, in which voltage is compared with pressure, and current with velocity. From the physical viewpoint, acoustic and mechanical impedance shows how difficult it is to “loosen” the system or the degree of the system’s incompressibility with vibrations.

2.2.2 Decay of Elastic Waves

A decrease in the plane harmonic wave amplitude as a result of its interaction with a medium takes place according to the law $e^{-\delta x}$, where x is the distance that the wave passes in the medium and δ is the damping coefficient. In what follows, the term “damping” will refer only to the wave amplitude decrease that is taken into account by an exponential multiplier, contrary to a decrease in the amplitude related to the wave front extension, e.g., in a spherical wave.

The value that is the reverse of the damping coefficient illustrates the distance at which the wave amplitude decreases e times, where e is the Napier number; therefore, the dimension of the damping coefficient is m^{-1} . In the literature [1], this unit is sometimes written as Np/m. However, this unit is not foreseen by the State Standard of Ukraine. The damping coefficient is often expressed by the number N of negative decibels, by which the wave amplitude decreases at a unit distance of its propagation $x = 1m \times N = 20 \lg e^{-\delta l} = -8.68 \text{ dB/m}$ ($1 m^{-1} = 1 \text{ Np/m} = -8.68 \text{ dB/m}$).

The damping factor consists of the coefficients of absorption δ_1 and dissipation δ_2 : $\delta = \delta_1 + \delta_2$. During absorption, a sound energy transforms to thermal, and during dissipation the energy remains sonic, but is emitted by a wave whose propagation is directional. Absorption is conditioned by ductility, elastic hysteresis (i.e., by a different elastic dependence during extension and compression), and heat conductivity. The last absorption mechanism is conditioned by the fact that the process of acoustic wave propagation is considered to be adiabatic. The extension

or compression of an elementary volume accompanied by the temperature alteration is so short that the process of temperature equalization cannot be taken into account. In fact, there is a heat conductivity that assists in the loss of vibration energy. There are also other mechanisms of absorption revealing themselves at frequencies higher than those used in technical diagnostics and nondestructive testing of components and structural elements.

The dissipation of waves occurs due to the medium heterogeneities whose wave resistance differs from a medium one; their sizes are commensurable with the wavelength. A difference in the wave resistances causes the reflection of waves. Small sizes and a large number of heterogeneities specify a statistical character of a dissipation process. Such heterogeneities can be represented, for example, by the inclusion of various types in alloys, solid particles, or bubbles of air in water. In gases and liquids, which do not contain foreign particles, there is no dissipation, and the damping is determined by absorption. The absorption coefficient is proportional to the square of frequency. Therefore, a value $\delta' = \delta/f^2$ is introduced as a characteristic of sound absorption in liquids and gases.

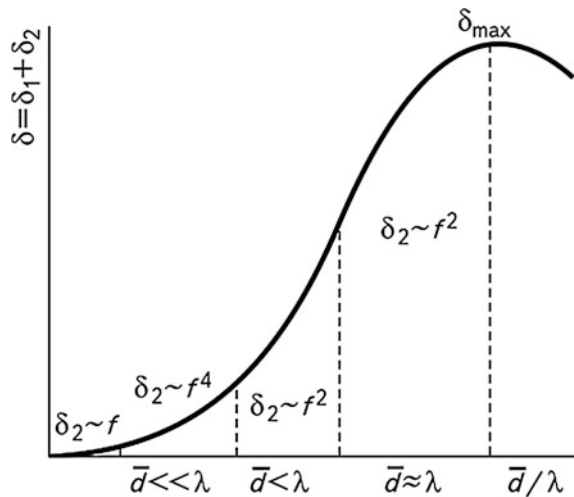
The absorption coefficient in solids is proportional to the frequency f (glass, biological tissues, metals, some plastics), or f^2 (rubber, majority of plastics). For the same medium, the absorption of transversal waves at $f = \text{const}$ is less than for longitudinal ones; this is because transversal vibrations are not conditioned by the change in a volume and there are no heat conductivity losses.

There is no dispersion in homogeneous amorphous solids such as glass and plastic. A weak dispersion in them can arise due to internal stresses that cause the change in elastic wave velocity and their refraction. In heterogeneous materials such as cast iron, granite, concrete, etc., dispersion is very large. Considerable dispersion is also observed in most metals, even at a high degree of homogeneity [1].

As is known, metals have a polycrystalline structure and consist of a great number of crystals (grains)—single crystals that are not clearly faceted. All crystals are most often randomly oriented; at the transition of elastic waves from one crystallite into another, their velocity can vary to a greater or lesser degree due to their anisotropy. As a result, a partial reflection, refraction, and transformation of wave types appears that determine the mechanism of dispersion. The greater the elastic anisotropy of crystals, the larger the dispersion. Anisotropy is also characterized by the parameter of elastic anisotropy. In a cubic crystal, it is a measure of relative resistance of crystals to two types of shear deformation. A large anisotropy is typical of copper, zinc, and austenitic stainless steel; a small elastic anisotropy is typical of tungsten and aluminum. Alpha iron and carbon steels belong to intermediate materials according to the value of elastic anisotropy and dispersion.

The value of the dispersion coefficient in a medium is greatly affected by the correlation of the average size of heterogeneities and the average distance between heterogeneities with the elastic wavelength. In metals, the medium parameter that significantly affects the dispersion of crystals is the average size of a particle \bar{d} . In

Fig. 2.14 Schematic dependence of the damping coefficient on the correlation of average grain diameter and the elastic wavelength



the case of $\bar{d} \gg \lambda$, coefficient δ_2 is proportional to f^4 (Rayleigh dispersion) (Fig. 2.14). Then, total damping is calculated by the equation

$$\delta = Af + Bf^4\bar{d}^3, \quad (2.31)$$

where A and B are the constants, and f is the frequency of vibrations. The term Af is caused by absorption, and it dominates at low values of f . In the region $4 \leq \lambda / \bar{d} \leq 10$, coefficient δ_1 is proportional to the product $\bar{d}f^2$.

In metals with different grain size, the power index at f varies from 2 to 4, and maximum damping is observed when $\lambda \approx \bar{d}$. In carbon steel, grains consist of a great number of fine plates of iron and cementite (Fe_3C). Their sizes are considerably smaller than the average size of grain \bar{d} . This is probably the reason that in a wide range of frequencies up to the values of $f = 4 \dots 5$ MHz in fine-grained carbon steels, the damping is determined by absorption, i.e., it is proportional to frequency. In austenite steel welded joints, the crystal orientation is ordered.

In general, a wave field generated by the AE source consists of elastic waves of different types: spatial longitudinal and transversal waves that, in their turn, generate the surface Rayleigh, Lamb, and other waves (Fig. 2.15). These waves propagate with various velocities and damp according to different laws. Thus, for instance, the damping of spatial longitudinal waves is proportional to R^{-2} , where R is the distance from the source to the observation point. Surface waves, such as Rayleigh and Lamb waves, damp proportionally to R^{-1} and are capable of carrying information on the AE source character at the distance greater than spatial waves.

In paper [10], a problem concerning the evaluation of elastic displacements in Rayleigh waves excited by the vertical harmonic point force source, which acts at a depth h under the surface of an elastic half-space, is solved. It shows that with the growth of h , the amplitude of waves decreases, and under condition

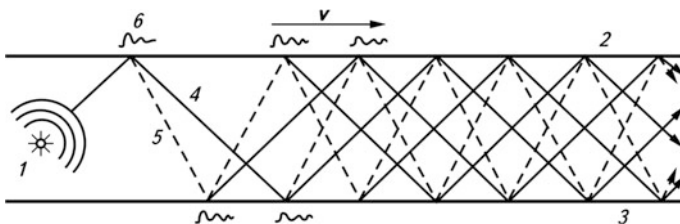


Fig. 2.15 Illustration of the elastic wave propagation in a plate (passing of one ray): 1 is a source, 2 is the upper surface of a plate, 3 is the bottom surface of a plate, 4 is a longitudinal wave, 5 is a transversal wave, 6 is a surface wave [9]

$h \geq (2 \dots 3)\lambda$ (λ is the wavelength), it tends to zero. The authors of [11] showed that due to the difference in the damping of spatial and surface waves, at large distances from the AE source, surface waves prevail even when the source mainly generates spatial waves. They stated the prevalence of that or other types of waves depending mainly on mutual locations of an AE source and an AET mounted on the IO. Therefore, in the case of their locating on one side of a plate, the Rayleigh wave prevails, while in other cases, when a source is inside a plate or when a source and a receiver are on different sides of the plate, the sequence of spatial longitudinal and transversal waves prevails in a waveform.

In paper [12], the propagation of elastic waves in pipe specimens of 17G1SU steel with various wall thicknesses was investigated using the method of “sounding.” Wide-band AETs were used for emitting and sensing elastic waves. To study the effect of water on the character of elastic waves propagation, experiments were performed on water-filled specimens. It was found that after filling the specimen with water, the velocities of elastic waves did not change, and only the dynamic parameters of the wave field underwent changes: the amplitude of spatial waves diminished, and vibrations arose between the appearance of longitudinal and transversal waves. The effect of the pipe specimens filling with water on the waveform was studied for various wall thicknesses h of specimens, taking into account the dimensionless parameter kh , where $k = 2\pi / \lambda$ is the wave number and λ is the wavelength. The physical essence of this parameter is that it determines the conditions of elastic wave propagation in pipe specimens: $kh \approx 1$ corresponds to the conditions of wave propagation in a plate, $kh \gg 1$ is for wave propagation in an infinite medium. The variation range of kh is from 2 to 10. At the values of $kh > 10$, the effect of water on the damping of elastic waves was not observed (Fig. 2.16).

Authors [12] suppose that the main contribution to the energy of wave package is given by Lamb waves, whose amplitude is by one order of magnitude higher than the amplitude of longitudinal spatial waves. The filling of a pipeline with water causes distortion of the wave forward front structure, producing an error during the AE signal location in the hydrotesting of pipelines.

Figure 2.17 shows the effect of pipe steel degradation in the feeding pipelines of supercritical pressure power units of thermal power stations on the damping of AE elastic waves. A knee pipe about 1130 mm long, cut out of the pipeline and not

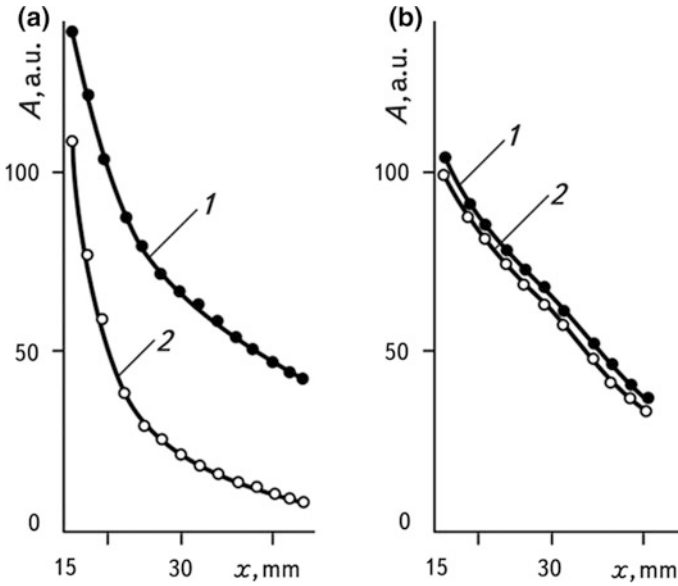


Fig. 2.16 Dependence of elastic wave amplitudes damping A (arbitrary units) on the value of kh and a passing distance x : **a** $kh = 2$; **b** $kh = 10$; 1 is for a specimen without water, 2 is for a specimen with water

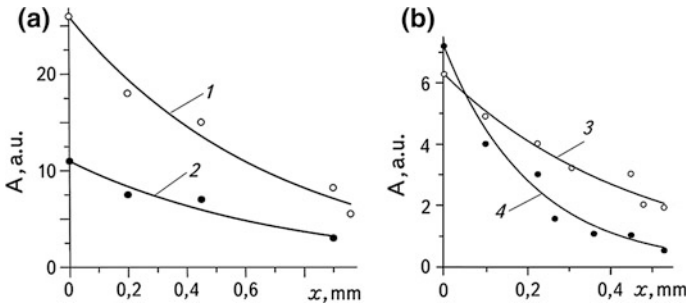


Fig. 2.17 Elastic AE waves damping while passing through the degraded material of a pipe bend made of 16GS steel, recorded by the resonance **(a)** and a wide-band **(b)** TAE: resonance frequency is 260 kHz (1); 320 kHz (2); 560 kHz (3); 810 kHz (4)

filled with the service environment, was investigated. For AE sounding, a probe-simulator of the AE pulses was used. The operating time of large-scale equipment was over 120,000 h.

Mechanical pulses were excited by electric rectangular pulses of voltage 12.5 V and frequency of 0.4 Hz. In order to select and record the AE signals, the AETs (see Chap. 1) were used as a set of serial AE devices that have various gain-frequency

Table 2.2 Damping of elastic waves in some liquids and in air at 20 °C [1]

Medium	Frequency f , MHz	Damping coefficient α/f^2 , $10^{14} \text{ s}^2/\text{m} = 10^5 \text{ m}^{-1} \text{ MHz}^{-2}$
Air	1.1...1.4	1670...2000
Water	7...250	2.5
Glycerin	0.5...4	250
Kerosene	6...21	170
Vinegar acid	0.5	9000
Oil (transformer)	1...5	130
Mercury	20...50	1.2...1.3
Alcohol ethyl	1...220	5.4

characteristics. They are mounted on the external surface of the pipe through a layer of acoustic transparent oil at certain distances from the stationarily installed sound simulator. The external diameter of the knee pipe was 410 mm, and its wall thickness was 55 mm.

As follows from the results of investigations (see also Table 2.2), the AE signals damp in a different manner depending on their frequency range. The design features of AET significantly affect this parameter as presented below:

Thus, the character of the wave field depends on the mutual arrangement of an AE source and a receiver, the source type and IO, frequency characteristics of the primary transducer. This means that in each case it is necessary to carry out experimental studies regarding the effect of the above-mentioned factors on the formation of the wave field that irradiates an expected or known AE source.

2.2.3 Diffraction of Elastic Waves

Diffraction (from the Latin “*diffRACTUS*” meaning “broken down”) of waves is a deviation of waves from the geometrical laws of propagation when interacting with obstacles. Hence, the diffraction of a sound (and ultrasound) is a deviation of the sound behavior from the laws of geometrical (ray) acoustics, conditioned by the wave nature of a sound. The elastic fields created by an initial wave diffraction on the obstacles are called “scattered” or “diffracted” waves [1].

We should consider the diffraction of elastic waves on the objects of a regular geometrical shape simulating real defects. Usually, it is very difficult to get the exact solution to most problems on elastic waves diffraction. Therefore, approximate methods are used for this purpose.

According to Young’s theory, the field that arises due to a wave diffraction is caused by the interference of waves that propagate according to geometrical laws as well as by diffracted waves that arise at the critical points with discontinuous boundary conditions. The boundaries of the obstacles—edges on their surfaces—are the locus of such points. According to the Fresnel theory, a diffraction field

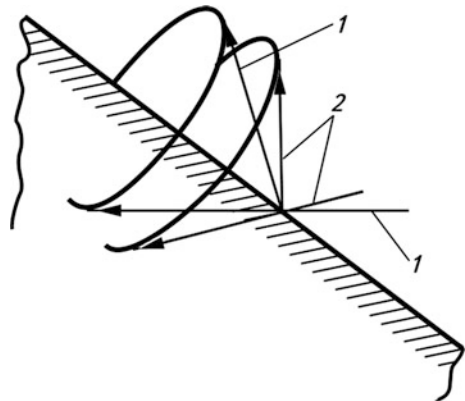
appears due to the action of fictitious secondary sources excited by an incident wave on the obstacle during the reflection or outside it (during passing). For the same conditions, the calculation results obtained using both methods coincide.

Diffraction on a slot edge and on a strip. An infinitely thin slot simulates real defects, such as lamination, extended crack, or faulty fusion, and its edge is the edge of the corresponding defect. The diffraction field calculation in this case is usually done using the Sommerfeld method, which is actually Young's theory development for plane obstacles. From each point of the edge (Fig. 2.18), a diffraction wave propagates as a cone, one of its generatrices being a continuation of the incident longitudinal wave ray; the transformed transversal wave forms another cone. Moreover, there are waves that spread along the slot surface. Amplitudes of all these waves are proportional to the amplitude of the incident wave, though by 1...2 orders less.

If a slot is not semi-infinite and is of a finite width, there are two edges, on each of which the diffraction waves similar to those considered in Fig. 2.18 appear. When a limited bunch of rays of an elastic wave covers both edges of the strip, and a mirror reflection from the strip does not reach the receiving transducer, its signal is determined by interference of diffracted waves from the edges. The points on the reflecting edges (similar to real defects), on which diffraction waves appear giving maximal contribution to the scattered wave field, are called "bright points."

Diffraction on a hollow disk. Small-sized, crack-like defects are simulated by a disk. A reflector is considered to be a hollow one if stresses on its boundaries are equal to zero. A problem on diffraction upon a disk is among the problems on the diffraction of elastic waves upon the small-sized objects in comparison with a wavelength. The exact solution of similar problems consists of expanding the incident and scattered waves into a series by functions close to the object shape. Oblate spheroidal functions are used for a disk, i.e., eigenfunctions of a wave equation in the system of oblate spheroidal coordinates that coincide with the disk surface.

Fig. 2.18 Formation of diffraction cones of longitudinal (1) and transversal (2) waves at an inclined incidence of a longitudinal wave on the slot edge



Expansion into a series is carried out, assuming that the value of $k_1 b < 2\pi$, where k_1 is the wave number for a transversal wave, and b is the disk radius. In the incident wave, coefficients of the series terms are known, while in the scattered longitudinal and transversal waves they are unknown. They are to be found from the boundary conditions: the normal and tangential stresses on a hollow disk surface are equal to zero. These conditions should be satisfied for the terms of identical powers in a series for the incident and scattered waves. Figure 2.19 shows the solution for perpendicular incidence of a longitudinal wave on a hollow disk in an aluminum body.

As we can see, the amplitude A_d of a scattered longitudinal wave at small angles of observation grows in a non-monotonous manner with the growth of $k_1 b$. At the same time, the directional diagram of the scattered wave narrows.

Diffraction on a cylinder, sphere, or ellipsoid. These objects simulate the real defects, such as pores, slag inclusions of various shapes, etc. They have a smooth convex surface. From the viewpoint of diffraction theory, they differ from the slot edge, strip, and disk by the absence of bright points, and the diffraction waves appear in every point on their surface.

A problem concerning diffraction on a cylinder is solved by expanding the scattered and incident wave potentials into a series by cylindrical functions. If kd is assumed to be of small value, where k is the wave number for longitudinal or transversal waves and d is the cylinder diameter, the solution is called a “long-wave approximation,” and if $1/kd$, it is considered to be a “short-wave approximation.”

An energy (ray) approximation ($d \gg \lambda$) yields the following expression for the amplitude of reverse reflection from a cylinder $B_c = 0.5\sqrt{d/\lambda}$. The long-wave approximation for $d \ll \lambda$ gives the value $B_c = 7.4(d/\lambda)^2$. The change in B_c for intermediate values of d/λ shows significant differences in the diffraction of various wave types (Fig. 2.20).

Fig. 2.19 Amplitudes of the longitudinal wave scattered on a hollow disk in aluminum at different observation angles θ [13]: *solid lines* correspond to a model for a solid; the *dashed line* is the Kirchhoff approximation for $\theta = 0$

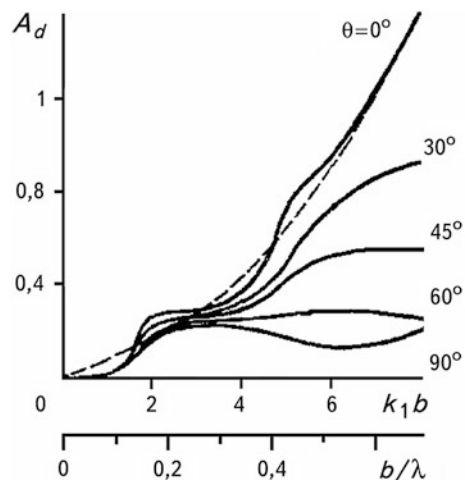
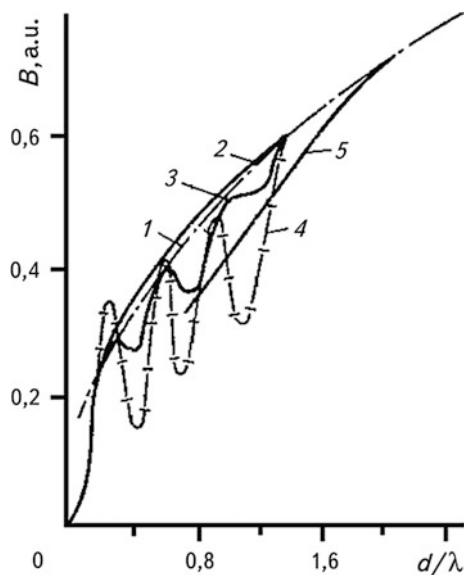


Fig. 2.20 Amplitude of a wave reflected from a hollow cylinder [13]



Curve 2 for a longitudinal wave rather precisely coincides with the energy theory data (curve 1) up to the values of $d/\lambda \geq 0.2$, and the reflection amplitude of a transversal wave coincides only up to $d/\lambda \geq 2$. At smaller value of d/λ , the theory predicts the occurrence of oscillations for a transversal wave reflection (curves 3, 4). These oscillations are especially large for waves with vertical polarization (perpendicular to the cylinder axis, curve 4). However, the results show (curve 5) that for a pulse character of irradiation theoretically calculated for continuous irradiation, there are either no oscillations of function 5 or they are very small, even though curve 4 is lower than for the energy theory.

The origin of oscillations and their smoothing can be explained by a short-wave approximation [13]. It is shown that in the case of a transversal vertical polarized wave incidence (Fig. 2.21), various types of waves are formed: transversal (Fig. 2.21a) and longitudinal (Fig. 2.21b), transformed from a transversal. A ray of the incident transversal wave that touches the cylinder surface excites the heterogeneous wave of a transversal type (Fig. 2.21c), which envelops the surface of the cylinder (enveloping wave).

Figure 2.21d shows the same wave that envelops the cylinder in a reverse direction (for other waves, which are examined below, the variants of reverse enveloping are not shown). These two waves generate transversal waves of sliding that starts from every point of a cylinder tangential to its surface.

A ray that falls on the cylinder surface at the third critical angle (Fig. 2.21e) generates a longitudinal enveloping wave (a head wave) which, in turn, generates the wave of sliding also of a transversal type that begins at the third critical angle. The ray of the incident transversal wave that passes close to the cylinder (Fig. 2.21f) creates an enveloping wave of the Rayleigh type, which also

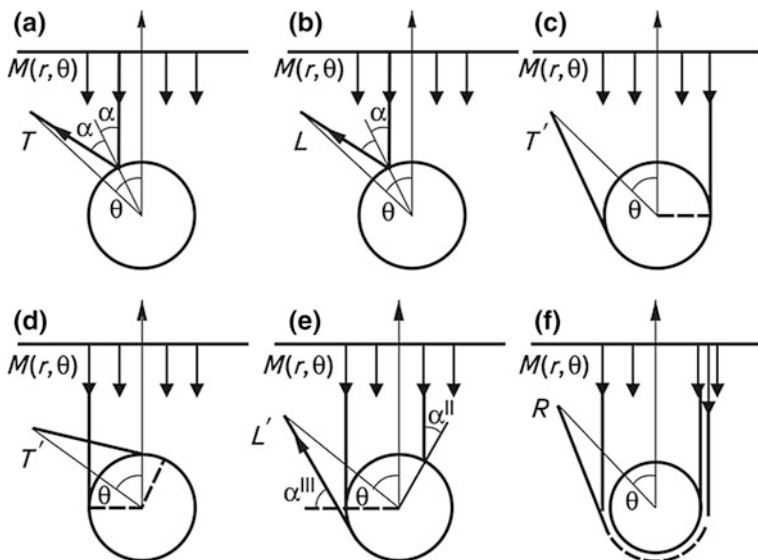


Fig. 2.21 Initiation and propagation of waves during diffraction of a transversal perpendicular polarized wave on a cylinder (a short-wave approximation)

re-irradiates the energy into space in the form of a transversal sliding wave, because it propagates along a concave surface.

Thus, except for the directly reflected elastic waves, three more transversal waves emerge in the observation point. These waves are generated by the enveloping waves of transversal, longitudinal and Rayleigh types. The amplitudes of the enveloping longitudinal waves are much lower than those of transversal and Rayleigh waves.

For a large diameter cylinder, the mirror reflected signal and a series of pulses of enveloping waves are clearly observed. With a decrease in the cylinder diameter, the pulses come closer, and they merge for the condition $d/\lambda \approx 1.5$, and their combined interference brings about oscillations. The condition of the lack of oscillations $d/\lambda > 1.5$ is close to the condition of coincidence of the experimental curve with the energy approximation curve ($d/\lambda \approx 2$).

Diffraction waves on a sphere are formed according to the same laws as on a cylinder. The difference is that during the longitudinal wave incidence on a sphere, the difference of amplitudes of the diffracted and mirror-reflected signals are fewer than for a cylinder. Due to an axial symmetry of the problem for a sphere, the rays that envelop a cavity at different directions arrive at the observation point simultaneously. This condition is satisfied only for a combined type of sounding ($\theta = 0$).

When a transversal wave falls on the sphere, the oscillations at various areas of its front are oriented differently with respect to the sphere surface; they can be expanded into vertical and horizontal polarized vibrations, the diffraction of which occurs by various laws. The intensive enveloping waves are typical only of the

vertical polarized vibrations, whose portion for a spherical object is less than for a cylinder.

For an elastic wave incidence on an ellipsoid or an elliptical cylinder, a diffraction field is formed; it has the features typical of diffraction on spatial objects, such as sphere or cylinder, and plane, such as disk or band. The prevailing type of diffraction depends on the degree of the ellipse oblateness determined by the ratio of the axes.

2.2.4 Refraction of Elastic Waves

Refraction—in the wide sense—is the same as the deflection of rays. Regarding acoustic waves, by refraction we mean a continuous variation of the acoustic ray direction in a heterogeneous medium. The velocity of the waves therein depends on the coordinates. This phenomenon is observed in a layered-heterogeneous and anisotropic medium, whose velocity varies according to a particular law. This medium is assumed to consist of an infinite number of infinite thin layers; in each layer, the elastic wave velocity is constant, but it varies step-wise at the boundaries of the layers. The sine law should be applied at the boundary of these two layers in order to determine the ray behavior: $\sin\alpha/c = \cos\gamma/c = \text{const}$, where $\gamma = 90^\circ - \alpha$ is the sliding angle. The variation of velocity c causes the deviation of the rays from their linear propagation direction, thus forming both acoustic shadows and zones of energy concentration in which acoustic surfaces arise.

We should mention some examples of the media having variable velocity of wave propagation, such as welded joints of austenitic steel, transversal isotropic non-metal materials, surface-hardened components, rolls of cold rolling, axes and bushes of some mechanisms, etc. A special heat treatment mode improves hardness of the surface layers while the internal layers of metal remain unhardened, ductile. They are often called “raw” metals. Thus, in the non-destructive testing of materials, components, and structures, specific features of a material structure should be considered.

2.3 AE Sources

Since most objects inspected by means of nondestructive testing and technical diagnostics are made of metallic alloys, the classification of the AE sources, which generate AE signals during initiation and propagation of a fracture therein, is of special interest to researchers. According to [14] they can be classified as follows: dislocation processes of metal plastic deformation, phase changes, second-phase particles fracture, magnetic effects, surface phenomena and external effects, and material failure. Let us briefly consider some of them, since they were described in the previous chapter.

Dislocation processes. It is shown in [15] that even in aluminum monocrystals of a high degree of cleanness, the AE was generated at stresses lower than the threshold of macroscopic yielding of metal. Later on, a group of researchers discovered a similar effect for other metals. Thus, in paper [16], the AE generation is recorded in dependence on the defect energy of a crystalline structure of copper alloy monocrystals. Using the terms of redistribution and motion of dislocations, the effect of Bauschinger that also causes the AE generation is explained [17]. It is thought that mobile screw dislocation generates AE during motion from one low-energy state to the other, at this point eliminating the oscillation in a lattice [18] that is confirmed by certain theoretical calculations [19–21]. It should be noted that the energy of an AE signal, which is conditioned by a single dislocation, is very low and is therefore difficult to detect. However, a cooperative motion of many dislocations was recorded without much difficulty by modern devices [22].

Annihilation of dislocations. In [23–25], models of the AE origin during annihilation of dislocations on the free surface or during their crossing the interface between two sections of the metal with a different elasticity module were described. The validity of these models is proved by the fact that AE irradiates during the electrochemical removal of the Al_2O_3 film from aluminum specimens [26].

Uniform motion of dislocation groups. There have been studies in which it has been indicated that the number of dislocations involved during co-operative motion varies from several hundred to a few thousand pairs [27, 28]. For the continuous AE, these values can be considerably smaller—from 10 to 100. There is a hypothesis that even irradiation by dislocations of discrete AE is conditioned by uniform motion of a great number of dislocations [29–31]. However, these statements have been corrected, and have shown that the AE is generated only during accelerated or decelerated motion of dislocation groups [22, 28, 32].

Action of a dislocation source. During the action of any dislocation source for a short interval of time on a slip plane in the same direction, a great number of similar dislocations is released and a dislocation avalanche is formed. In [22, 33] it is established, from the analysis of literary sources, that the action of the Frank-Read source causes the AE from LiF monocrystals and metals. It is emphasized that on the silicon steel, the sources of dislocations appear at stresses lower than the macroscopic elasticity limit. The same is set for monocrystals of copper and zinc.

Dislocation breaking from the pinning points [22]. There are models in which the AE bursts are explained by the concepts of sudden pressure (avalanche) of newly formed free dislocations [33–35]. This was experimentally confirmed in papers [36–38] on various metals. For the development of the mentioned concepts, a hypothesis [39] was proposed, according to which dislocations move in the slip bands packages, each of them having a certain number (n) of dislocations. With the beginning of an unsteady plastic flow, the n is large and the AE irradiation is substantial. The behavior of other AE parameters can be explained by the fact that the density of dislocation packages is described by the Weibull distribution as a function of strain.

Formation of slip bands. Studies are known in which the dependences between the slip bands' initiation and the formation of discrete AE in Mg, Cu, and Fe

monocrystals were investigated [35]. It was found that the appearance of the first AE pulse corresponds to the origination of the first slip band. The authors believe that the process of formation of the first slip band is simulated by a primary plastic flow caused by a creeping avalanche. It should be noted that such a model, although having the right to exist, is very blurred.

Grain boundary slipping. Since Kaiser's studies [40], a hypothesis has been proposed that says that AE is conditioned by the motion of grain boundaries. However, modern achievements in AE studies refute these assertions, leaving them partly for description of the AE parameters generated in the case of deformation of lead and its alloys. Thus, we can disregard the viewpoint that the mechanisms of grain boundaries sliding are crucial or important sources of the AE [14].

Microvoids coalescence. It is commonly known that development of plasticity in metals includes the process of the formation of cavities or pores and their further development and coalescence. The mechanism of final coalescence can cause a spontaneous failure of ligaments between cavities. In this case, the AE pulses are also generated, and especially considerable AE arises during ligament breakage [22].

Phase transformation. A sudden transition of one metastable phase into another is, possibly, the first case of AE best revealed by man. The famous "cry of tin" [14, 22] is the most widely used example to illustrate the processes of AE generation. Such processes are basic AE sources in some metals under certain conditions of their deformation, and rarely occur when other AE sources are comparatively small. In this case, AE is an exceptionally accurate and useful factor for investigating transformation processes.

Strain twinning. The twinning of tin and zinc is the phenomenon known in metallurgy, which in the case of tin loading generates such AE that it is usually perceived by the human ear as a series of crunches [41]. Similar effects of AE generation are observed in titanium [42] and its alloys, and in zirconium [43] and zinc [44]. This proves that in these metals, the twinning is the basic source of AE, while the remaining mechanisms, including dislocation sliding, are the secondary ones.

Elastic twinning. The AE pulse [45] accompanies the initiation and disappearance of a single twin induced by the application of stresses to a calcite. It was established in [14] that the initial stages of a twin development and sliding are very similar processes. Therefore, the same model can be used to explain them [45]. This assumption today is insufficiently grounded to provide a clear distinguishing of the mentioned above mechanisms as the AE sources.

Twinning expansions. The AE was observed in zirconium with the expansion of twins [39]. The phenomenon has not yet been studied well enough and needs special investigations.

Martensite transformations. The AE appears during transformation of austenite into martensite, bainite, pearlite, and ferrite [46]. The most important characteristics of the AE parameters are as follows:

- The AE beginning coincides with the first martensite formation;

- The cumulative count of the AE attains the maximum at a martensite final temperature, i.e., the AE accompanies a transitional process;
- The cumulative count of AE increases with an increase of carbon content;
- The count rate is maximal at the temperature lower by 50 °C than the temperature of the beginning of martensite transformation. Thus, this temperature can be evaluated by the AE data;
- The cumulative count of AE per volume unit of martensite formation is very sensitive to carbon content, which is determined by the martensite morphology; and
- The lamellar formations of martensite irradiate the AE of a greater energy than the strip martensite. It is not caused simply by the relative value of the volume of the formations, but can be caused by high rates of a lamellar martensite growth.

These ideas are confirmed in papers [47–49], where the alloys of non-ferrous metals and steel were experimentally investigated. Some metastable steels irradiate AE at relatively high and uniform rates of plastic deformation [50–53]. This formed a basis for the study of the processes of martensite formation using the AE parameters.

Beinitic, eutectoid reactions and other phase transformations are also accompanied by the AE [54] generation, which to some extent can be used for their qualitative or quantitative estimation.

Fracture of secondary phase particles. In many cases, metal ductility depends on the fracture easiness of either a particle or the boundary between the particle and the matrix, as well as on the volume fraction of these particles, their distribution, shape, etc. Therefore, it is reasonable to expect that such failures are accompanied by AE, as they are the processes of local stresses relaxation. Every industrial alloy has its inherent concentration of the secondary phase particles. It can change from extremely fine-grained required precipitations in, for instance, areas of recrystallization in duralumin, to relatively large, undesirable inclusions, such as silicates in steels. The nature, size, amount, and the effect of every particle varies within a wide range, hence the AE generation is specific for every metal.

Non-metal inclusions in steels. In steels, the amount of inclusions reaches $10^{12} \dots 10^{15}$ per tone of metal for relatively pure grades. Their composition, sizes, shape, properties, etc., are usually different, but they can be grouped as aluminates, silicates, or sulfides. The failure of such inclusions under mechanical stresses is accompanied by the AE [28, 53]. This occurs at almost all stages of deformation. In study [54], the mechanisms related to inclusions are distinguished as [54]:

- Decohesion of MnS streaks along the interface that is located parallel to the rolling plane;
- Fracture of the silicates streaks or MnS across or along the direction of rolling;
- Decohesion of MnS and failure of SiO_2 particles of a spherical shape;
- Failure of the piled-up dislocation groups at an inclusion during the break or decohesion of the last; and
- Friction between the surfaces of the failed brittle particles.

Carbides in steels. Some authors have devoted a number of papers to the problem of carbide fracture in steels [54]. In some of the papers it is proved that the majority of AEs are caused by failure of carbide plates in pearlite or at the ferrite grain boundaries. However, spheroidized carbides in pearlite emit a relatively low amount of AES. There is a scientifically sound assertion that grain boundary films fail under very insignificant deformations. Plates of pearlite fail at greater deformations depending on their size, and spheroidal particles fail within the strain range from 30 to 40%. There is a tendency of these processes to depend on the size, shape, and orientation of the particles in a metal.

Precipitations in aluminum alloys. The action of the AE sources in aluminum alloys is described in detail in [55], and the appearance of two AE peaks is vividly illustrated in paper [37], in which the aluminum alloy went through the yielding point at the early stages of deformation. It is shown that the first AE peak is caused by dislocation mechanisms, and the second by failure of the fine brittle intermetallic inclusions. These peaks split under the action of tensile strain, which was later verified by other researchers [54]. It is seen from the above that AE in most aluminum alloys is mainly the result of the fracture of solid particles. It should be emphasized that a dependence of fracture toughness was found on the brittle particles' location in front of the macrocrack tip in aluminum alloy.

Fibers and fibrous composites. Mechanisms of initiation and development of fracture of different fibers and fibrous composites are described in detail in [56]. The AE caused by fiber failure are highly energetic and are well detected by equipment. Although individual features of the AE generation in materials differ, in the case of composites it is possible to quite easily distinguish the AE sources related to the material fracture mechanisms by the AE parameters [56].

Slag inclusions in welded joints. The fracture of slag inclusions takes place during a weld cooling, which is accompanied by the initiation of mechanical stresses. As a result, the AE emits (a detailed description is given in [57]).

Magnetic effects. Ferromagnetic materials subjected to mechanical stresses tend to order their domains so that the magnetostriction deformation is in the direction of the applied loading. The Barkhausen effect is observed in iron alloys caused by the turning of the domain walls. It is known [58–61] that such motion of domain walls under tensile deformation causes the AE generation during the elastic deformation of the material. This phenomenon forms the basis for investigations of a number of structural materials in order to determine their physical properties [54]. Recently, the methods of AE investigations, comprising the Barkhausen effect, have been more widely used in the non-destructive testing of products and constructions.

Surface effects. The AE is also generated during cracking or delamination of oxide layers from the surface of steel specimens. In other cases, the AE sources are also the traces of sliding lines; the formation of dimples that collapse as well as pores, cracks, or dislocations that come out on the surface are considered to be the AE sources [54]. It is also known [62–64] that the processes of surface friction are accompanied by the AE.

Fracture of materials. Fracture is a complex process that includes a number of possible mechanisms and phenomena that have already been described above as the

AE sources. It mainly concerns the formation and development of the processes of plastic deformation in front of the crack tip. Therefore, when investigating the AE during the fracture of metals, it is essential to clearly define the origin of AE signals, and to find their correspondence to proper mechanisms that occur in a metal at different stages of fracture (see Chap. 1). The most important of them are related to the processes that accompany metal plastic deformation, such as dislocation processes, initiation, and propagation of pores, inclusion failure, and cracking.

The start of a macro-crack and the stages of a macro-crack sub-critical growth are accompanied by discrete high-amplitude AE, which is described in detail in Chap. 5 of this monograph. These fracture stages have been quite well studied, which is attested to by the research results published in a number of monographs [65–71] and review papers [72–78]. Here we will mention only a few of them:

Stress corrosion cracking. This phenomenon is one of the most active AE sources. A number of high-strength steels under stress corrosion cracking in an NaCl environment generate the AE with energy that is proportional to the crack area. The AE during intergranular fracture is energetically higher than during transgranular cracking. A similar situation is observed for stress corrosion cracking of coarse-grained and fine-grained steels [54, 79]. The AE method presented above is successfully used for the estimation of the threshold stress intensity factor under stress corrosion cracking of steels [80, 81].

Hydrogen embrittlement. During the fracture of a hydrogen-induced embrittlement of steel, a high amplitude level of the discrete AE is also observed [54, 80, 82–84]. The energy level of AE signals during such processes is higher than under stress corrosion cracking. Taking this into consideration, the AE method has proved to be very useful in detecting and observing the delayed fracture in forgings and welded joints [57]. The studies have shown a good correlation between the rate of hydrogen-induced cracking and the AE parameters [85–87].

Summing up the above, Table 2.3 presents the most typical AE sources during initiation and development of fractures in metals.

It is worth noting that the AE is also generated during fracture initiation and propagation in other non-metal materials. Numerous publications in the world's scientific journals are devoted to this phenomenon. Since there is a certain analogy in the propagation of elastic waves and in the AE sources action, we will not discuss it.

When conducting non-destructive testing of objects in industrial or in field conditions, the sources of AE can be gusts of wind, rain, snow, hail, etc., that cause the propagation of elastic AE waves as noise or background level of noises. This phenomenon should be taken into account when interpreting the results of non-destructive testing and diagnostics of the state of products and constructions. In Tables 2.4 and 2.5, the quantitative AE parameters and ranges of their variations are presented for the most characteristic sources of AE.

Table 2.3 Some AE sources in metals

Group	Source	Comment
1	2	3
Dislocation mechanisms under plastic deformation	Motion of one dislocation ¹	Below the susceptibility threshold of serial equipment
	Annihilation of dislocations on the free surface ²	
	Self-annihilation of a couple of dislocations ³	Below the susceptibility threshold of serial equipment
	Fracture of a dislocation loop ⁴	Below the susceptibility threshold of serial equipment
	Uniform motion of a group of dislocations ⁵	Below the susceptibility threshold of serial equipment
	Action of the Frank-Read source	Possible source of AE, but not prevailing
	Action of the source of dislocations located at the grain boundary	Possible source of AE, but not prevailing
	The avalanche of the dislocation—dipoles capture phenomena that occur at the grain edge	Possible source of AE applied in fatigue testing at small deformation
	Non-fixing of dislocations or breaking of dislocations ⁶	Source is proved soundly
	Formation of a slip band	It is not the basic mechanism
Phase changes	Slipping in the grain lattice	Possible only in lead alloys at 20 °C
	Deformation at which twinning takes place	Possible source in certain metals and alloys
	Formation of elastic twins	
	Extension of twins	Possible, but does not refer to metals
	Martensite transformations	Steel, brass
	Beinitic resistance in steels	Requires investigations
Particles of the second phase	Phase transformations in tin	Not identified
	Non-metal inclusions in steel	Obviously play very important part in industrial steels
	Carbides in steels	Obviously play an important part in industrial steels
	Phase precipitation in aluminum alloys	Dominant source
	Fibers in composites	Dominant source
Magnetic effects	Slag inclusions in seals	Play an important part
	Motion of magnetic domain wall (the Barkhausen effect) Superconductivity	Very important, but not in most cases
Surface effects	Surface oxides	A source is very effective, sometimes is used successfully
	Surface coatings	

(continued)

Table 2.3 (continued)

Group	Source	Comment
1	2	3
Fracture	Formation of cavities	Important part in fatigue testing
	Failure of bonds	Dominant sources of AE
	Breakage of surfaces	High-energy sources of AE
	Micro-crack formation	Plays an important part in most cases, including corrosion and welding
	Crack propagation	
	Stress corrosion	
	Hydrogen embrittlement	

Energy of the AE source [J]: ¹10⁻²³; ²4 × 10⁻¹⁸; ³5 × 10⁻²⁴; ⁴≈10⁻²⁴; ⁵10⁻²³; ⁶10⁻¹⁹

Table 2.4 Ranges of change in some AE parameters during its fail-safe recording on IO

Parameter	Range of the parameter change		Notes
	Electric signal	Mechanical signal	
Cumulative count of AE	0...10 ⁷ counts	–	During the time of specimen tension to failure
Count rate	0...10 ⁵ counts/s	–	
Amplitude	10 ⁻⁷ ...10 ⁻² V	10 ⁻⁷ ...10 ⁻¹⁴ m	Single signal of discrete AE
Signal energy	10 ⁻¹¹ ...10 ⁻⁵ J	–	
Pulse duration	10 ⁻⁴ ...10 ⁻⁸ s	–	–

Table 2.5 Parameters of acoustic emission signals for some sources [57]

Type of source	Amplitude or pulse energy of the AE, J	Signal duration, μs	Width of a signal spectrum, MHz
Dislocation source of Frank-Read	(10 ⁻⁷ ...10 ⁻⁸)G*	5...50 × 10 ³	≤1
Annihilation of dislocations of length of 10 ⁻⁶ ...10 ⁻⁴ cm	4(10 ⁻¹⁸ ...10 ⁻¹⁶)	5 × 10 ⁻⁵	Hundreds
Micro-crack initiation	10 ⁻¹⁰ ...10 ⁻¹²	10 ⁻³ ...10 ⁻²	≤50
Disappearance of twins of volume ≈1 mm ³	10 ⁻² ...10 ⁻³	1 × 10 ⁴	–
Plastic deformation of a volume ≈10 ⁻³ mm ³	1 × 10 ⁻⁴	≤1 × 10 ³	≤0.5
Energy of thermal noises	4.2 × 10 ⁻⁴ J/Hz	–	Uniform spectrum to 10 ⁷

Taking into consideration the factors that cause the AE origination, and according to the characteristics of a qualitative effect on the formation of AE sources, they can be grouped as follows.

Factors that cause the initiation of the AE signals with large amplitude	Factors that cause the initiation of the AE signals with small amplitude
• High breaking strength	• Low breaking strength
• High rate of loading	• Low rate of loading
• Anisotropy	• Isotropy
• Heterogeneity	• Homogeneity
• Dense materials	• Porous materials
• Twinning	• Absence of twinning
• Fracture along the weld plane (neck of welding)	• Shear deformations
• Low temperatures	• High temperatures
• Materials with cracks	• Materials without cracks
• Martensitic phase transformations	• Diffusive controlled transformations
• Cracks propagation	• Plastic deformation
• Cast structures	• Forged structures
• Size of a large grain	• Size of a small grain

Thus, in summary, it is possible to state that various elastic waves initiate and propagate in materials under fracture initiation and further propagation. Their sources are also formed through a variety of mechanisms. Therefore, when using non-destructive test methods based on the AE phenomenon, it is necessary to take this variability into consideration and choose the optimum facilities as well as the modes of selection and recording of the AE signals.

References

1. Yermolov IN et al (1991) Akusticheskoye metody kontrolya (Acoustic methods of testing). In: Nondestructive testing, vol 2. Vysshaya Shkola, Moskva
2. Novatskiy V (1975) Teoriya uprugosti (Elasticity theory). Mir, Moskva
3. Aki A, Richards PD (1983) Kolichestvennaya seysmologiya. Teoriya i metody (Qualitative seismology. Theory and methods), vol 1. Mir, Moskva
4. Chebanov VY (1986) Lazernyy ul'trazvukovoy kontrol' materialov (Laser ultrasonic testing of materials). Izdat. Leningrad. U-ta, Leningrad
5. Mazon U, Tereton R (eds) (1973) Fizicheskaya akustika (Physical acoustics), vol 6. Mir, Moskva, p 132
6. Viktorov IA (1981) Ul'trazvukovye poverkhnostnye volny v tverdykh telakh (Ultrasound surface waves in solids). Nauka, Moskva
7. Krasilnikov VA, Krilov VV (1984) Vvedenie v fizicheskuyu akustiku (Introduction to physical acoustics). Nauka, Moskva

8. Brehovskikh LM, Godin OA (1989) *Akustika sloistych sred* (Acoustics of layered media). Nauka, Moskva
9. Birchon D (1979) Cries of stress. *Spectrum* 165:5–8
10. Budenkov GA et al (1981) Vozbuzhdenie voln Releya istochnikom tipa garmonicheskoy sosredotochennoy sily, deystvuyushey nad poverchnost'yu uprugogo poluprostranstva (Excitation of the Raleigh waves by a source of the harmonic concentrated force type acting over the surface of an elastic half-space). *Defektoskopia* 2:37–42
11. Vakshys E, Botava E (1982) Rasprostraneniye uprugich voln pri akustiko-emissionnom kontrole yadernykh reaktorov (Propagation of elastic waves during acoustic emission testing of Nuclear reactors). *Materialy 10-y Mezhdunarodnoy konferentsii po nerazrushayuschemu kontrolyu* (Proceedings of the 10th international conference on nondestructive testing), vol 4. Moscow, pp 33–37
12. Stryzhkov SA, Vynkler ON (1988) Issledovanie kharaktera rasprostraneniya uprugich kolebaniy v trubakh pri akustiko-emissionnom kontrole (Investigation of the character of elastic vibrations propagation in pipes during acoustic emission testing). In: *Nerazrushayushchiy kontrol' i diagnostika truboprovodov* (Nondestructive testing and diagnostics of pipelines). Nauka, Moskva, pp 15–21
13. Alioshyn NP (ed) (1989) *Metody akusticheskogo kontrolya metallov* (Methods of acoustic testing of metals). Mashynostroyeniye, Moskva
14. Jaffrey D (1979) Sources of acoustic emission (AE) in metals. A review. *Aust Chem Eng* 20 (9–10): 9–17, 21
15. Skalskiy VR, Andreykiv OY, Serhiyenko OM (2003) Doslidzhennya plastychnogo deformuvannya materialiv metodom akustichnoyi emisiyi. Oglyad (Investigation of the materials plastic deformation by the acoustic emission method. A review). *Fizyko-chimichna mehanika materialiv* (Physico-chemical mechanics of materials) 1:77–94
16. Schofield BH (1961) Acoustic emission under applied stress. Contract AF-33(616)—5640. Progress Report, vol 11. Lessells and Associates, Inc., Boston, Massachusetts
17. Hatano H (1976) Strain-rate dependence of acoustic-emission power and spectra in aluminum alloys. *J Appl Phys* 47(9):3873–3876
18. Siegel E (1977) Burst acoustic emission during the Bauschinger effect in FCC and HCP metals and alloys. *Acta Metall* 25(4):383–394
19. Eshelby JD (1949) Dislocations as a cause of mechanical damping in metals. *Proc Roy Soc L A* 197(1050):396–416
20. Eshelby JD (1956) A continuum theory of lattice defects. *Prog Solid State Phys* 3:79–85
21. Kosakevych AM, Margvelashvili IG (1967) Izlucheniye elektromagnitnykh i zvukovykh voln dislokaziyey, ravnomerno dvizhusheysya v ionnom kristalle (Irradiation of electromagnetic and sound waves by dislocation moving uniformly in ion crystal). *Izvestiya AN SSSR. Seriya Fizika* (Reports of the Academy of Sciences of the USSR. Ser. Physics) 31(5):848–850
22. Cortellazzi G et al (1973) A lattice-dynamics approach to the acoustic signal by a uniformly moving dislocation. *J Appl Phys* 44(4):1518–1523
23. Natsyk VD (1968) Izlucheniye zvuka dislokaziyey, vychodyashey na poverchnost' kristalla (Irradiation of a sound by dislocation, appearing on the crystal surface). *Pisma zhurnal eksperimentalnoi i tekhnicheskoy fiziki* 8(6):324–328
24. Graff KF (1975) *Wave motion in solids*. Clarendon Press, Oxford
25. Natsyk VD, Chyshko KA (1972) Zvukovoe izlucheniye pri annigilyazii dislokaziy (Sound irradiation caused by annihilation of dislocations). *Fizika tverdogo tela* (Phys Solids) 14 (11):3126–3132
26. Schofield BH (1972) Research on the source and characteristics of acoustic emission. In: *Acoustic emission*. ASTM STP 505. American Society for Testing and Materials, Philadelphia, Pennsylvania, pp 11–19
27. Kim HC (1976) Atomic structure and mechanical properties of metals. In: *Proceedings of the International School of Physics "Enrico Fermi"*, 8–10 July 1976
28. Mirabile M (1975) Acoustic emission energy and mechanisms of plastic deformation and fracture. *Non-Destr Test* 8(2):77–85

29. Dunegan HL, Harris D, Tatro CA (1968) Fracture analysis by use of acoustic emission. *Eng Fract Mech* 1(1):105–122
30. Gillis PP (1972) Dislocation motions and acoustic emission. In: *Acoustic emission*. ASTM STP 505. American Society for Testing and Materials. Philadelphia, Pennsylvania, pp 20–29
31. Malen I, Bolin LA (1974) Theoretical estimate of acoustic-emission stress amplitudes. *Physica Status Solidi (B) Basic Res* 61(2):637–645
32. Kim HC (1975) Characterization of mechanical properties by acoustic emission using an energy criterion. In: *Ultrasonic symposium proceedings*. Institute of Electrical and Electronics Engineers, Inc., Los Angeles, California. 22–24 Sep 1975
33. Sedgwick RT (1968) Acoustic emission from single crystals of LiF and KCl. *J Appl Phys* 39(3):1728–1740
34. Day CI (1969) An investigation of acoustic emission for defect formation in stainless steel weld coupons. Richlai, Washington
35. Fisher RM, Lally LS (1967) Microplasticity detected by an acoustic technique. *Canad J Phys* 45(2):1147–1159
36. James DR, Carpenter SH (1971) Relationship between acoustic emission and dislocation kinetics in crystalline solids. *J Appl Phys* 42(12):4685–4697
37. Carpenter SH, Higgins FP (1977) Sources of acoustic emission generated during the plastic deformation of 7075 aluminum alloy. *Met Trans A* 8A(10):1629–1632
38. Carpenter SH (1976) Report No. AFML-TR-75–212. Rockwell Science Center, Thousand Oaks, Jan 1976
39. Tetelman AS (1972) Acoustic emission and fracture mechanics testing of metals and composites. In: *Proceedings of the U.S.–Japan Joint symposium on acoustic emission*, 4–6 July 1972
40. Kaiser J (1953) Erkenntnisse und Folgerungen aus der Messung von Gerauschen bei Zugbeanspruchung von Metallischen Werkstoffen. *Arch Eisenhüttenwesen* 1/2:43–45
41. Woodward B, McDonald NR (1975) Flaw identification using acoustic emission. In: *Proceedings of the 3rd international conference on structural mechanics in reactor technology*, London, England, 1–5 Sep 1975
42. Tanaka H, Horiuchi R (1975) Acoustic emission accompanied by twin formation in titanium and titanium alloy. *Bull Inst Space Aeronaut Sci Univ Tokyo* 11(2A):427–435
43. Toronchuk JP (1977) Acoustic emission during twinning of zinc single crystals. *Mater Eval* 35(10):51–53
44. Boiko VS, Gaber RI, Kryvenko LF (1974) Zvukovaya emissiya pri annigilyazii dislokazionnogo skopleniya (Sound emission during annihilation of dislocation group). *Fizika tverdogo tela (Phys Solids)* 16(4):1233–1235
45. Boiko VS et al (1970) Zvukovoe izluchenie dvoynikuyuschich dislokaziy (Sound irradiation of twinning dislocations). *Ibid* 12(6):1753–1755
46. Speich GR, Schwaebel AJ (1975) Acoustic emission during phase transformation in steel. In: *Spanner JC, McElroy JW (eds) Monitoring structural integrity by acoustic emission*, ASTM STP 571. Pennsylvania, Philadelphia, pp 40–58
47. Speich GR, Fisher RM (1972) Acoustic emission during martensite formation. *Acoustic emission*, ASTM STP 505. American Society for Testing and Materials. Philadelphia, Pennsylvania, pp 140–151
48. Liptai RG, Dunegan HL, Tatro CA (1969) Acoustic emission generated during phase transformations in metals and alloys. *Int J Nondestr Test* 1:213–221
49. Pascual R et al (1975) Acoustic emission and the martensitic transformation of β -brass. *Scripta Metall* 9(1):79–84
50. Hartman WF, Kline RA (1977) Variations in frequency content of acoustic emission during extension of HF-I steel. *Mater Eval* 35(7):47–51
51. Palmer IG, Holt J, Goddard DJ (1974) Acoustic emission measurements on type 316 stainless steel. In: *EWGAE—ISPRA: proceedings of third meeting of the european working group on acoustic emission*, ISPA, Italy, 25–26 Sept 1974, pp 11–26

52. Ono K (1974) Acoustic emission and microscopic deformation and fracture processes. In: Proceedings of the second acoustic emission symposium, Japan, 2–4 Sep 1974, pp 1–63
53. Tetelman AS, Chow R (1972) Acoustic emission testing and microcracking processes. In: Acoustic Emission, ASTM STP 505. American Society for Testing and Materials. Philadelphia, Pennsylvania, pp 30–40
54. Jaffrey D (1979) Sources of acoustic emission (AE) in metals. A review. Australian Chemical Eng 20(11):9–11, 20(12):13–17
55. Andreykiv OYe, Skalskiy VR, Serhiyenko OM (2001) Vyznachennya ob'yemnoyi poshkodzhennosti alyuminiyevykh splaviv za sygnalamy akustichnoyi emisiyi (Determination of volume damaging of aluminium alloys by the acoustic emission signals). Fizyko-khimichna mechanika materialiv (Physicochem Mech Mater) 3:77–90
56. Andreykiv OY, Skalskiy VR, Serhiyenko OM (2001) Akustiko-emisiyni kryteriyi dlya ekspres oznaky vnutrishnich poshkodzhenn' kompozitnich materialiv (Acoustic-emission criteria for express estimation of internal damages in composite materials). Ibid 1:91–100
57. Ivanov BI, Belov VM (1981) Akustiko-emissionnyy kontrol' svarki i svarynykh soedineniy (Acoustic emission testing of welding and welded joints). Mashynostriyenie, Moskva
58. Shibata M, Ono K (1981) Magnetomechanical acoustic emission—a new method for non-destructive stress measurement. NDT Int 14(5):227–234
59. Lindgren M, Lepisto T (2000) Application of a novel type Barkhausen noise sensor to continuous fatigue monitoring. NDT & E Int 33(6):423–428
60. Song YY et al (2000) The effect of microstructural changes on magnetic Barkhausen noise and magnetomechanical acoustic emission in Mn–Mo–Ni pressure vessel steel. J Appl Phys 87(9):5242–5244
61. Park DG et al (1999) Nondestructive evaluation of irradiation effects in RPV steel using Barkhausen noise and magnetoacoustic emission signals. J Magn Magn Mater 196–197:382–384
62. Schwalbe H-J, Bamfaste G, Franke R-P (1999) Non-destructive and non-invasive observation of friction and wear of human joints and of fracture initiation by acoustic emission. J Eng Med 213(1):41–48
63. Baranov VM, Kudryavtsev EM, Sarychev GA (1997) Modelling of the parameters of acoustic emission under sliding friction of solids. Wear 202(2):125–133
64. Jiaa CL, Dornfeld DA (1990) Experimental studies of sliding friction and wear via acoustic emission signal analysis. Wear 139(2):403–424
65. Druillard TF (1979) Acoustic emission. A bibliography with abstracts. IFI/Plenum, New York
66. Spanner JC (1974) Acoustic emission: technique and applications, vol 12. Intex publ, Co, Evanston, Illinois
67. Williams RV (1980) Acoustic emission. Adam Hilger, Bristol
68. Vakar KB (1980) Akusticheskaya emissiya i ee primenenie dlya nerazrushayushchego kontrolya v yadernoy energetike (Acoustic emission and its application for nondestructive testing in nuclear power generation industry). Atomizdat, Moskva
69. Andreykiv AY, Lysak NV (1989) Metod akusticheskoy emissii v issledovanii prozessov razrusheniya (A method of acoustic emission in investigation of fracture processes). Naukova dumka, Kiev
70. Collacott R (1989) Diagnostika povrezhdeniy (Damages diagnostics) (trans: Babaievskiy PG). Mir, Moskva
71. Stryzhalo VA et al (1990) Prochnost' i akusticheskaya emissiya materialov i elementov konstruktsiy (Strength and acoustic emission of materials and structural elements). Naukova Dumka, Kiev
72. Dunegan HL, Tatro CA (1971) Acoustic emission effect during mechanical deformation. In: Bunshan RF (ed) Techniques of metals research, vol 5(2/12). Interscience, New York, pp 273–312
73. Tanaka Kh, Horiyui Kh, Sakakibara Y (1977) Akusticheskaya emissiya pri plasticheskoy deformatsii – metallovedcheskie faktory (Acoustic emission under plastic deformation—material science factors). Kindzoku dzajre 13(2):21–26

74. Wadley HNG, Scruby CB, Speake JH (1980) Acoustic emission for physical examination of metals. *Int Met Rev* 25(2):41–64
75. Ono K (1994) Trends of recent acoustic emission literature. *J Acoust Emis* 12(3/4):177–198
76. Skalskiy VR, Demchyna BG, Karpukhin II (2000) Ruynuvannya betoniv i akustichna emisiya (Oglyad). Povidomlennya 1. Stachne navantazhennya i vplyv temperaturnogo polya (Concrete fracture and acoustic emission (A review). Report 1. Static loading and effect of temperature field). *Tekhnicheskaya Diagnostika i Nerazrushyushchii kontrol* (Technical diagnostics and nondestructive testing) 1:12–23
77. Skalskiy VR, Demchyna BG, Karpukhin II (2000) Ruynuvannya betoniv i akustichna emisiya (Oglyad). Povidomlennya 2. Koroziya zalizobetonu. Aparaturni zasoby. AE – kontrol' ta diagnostyka budivel'nykh sporud (Concrete fracture and acoustic emission (A review). Report 2. Corrosion of the reinforced concrete. Equipment. AE examination and diagnostics of building constructions). *Ibid* 2:9–27
78. Andreykiv OY et al (2000) Rozvytok doslidzhen' prozesiv ruynuvannya iz zastosuvannyam yavischa akustichnoyi emisiyi u FMI Im. G.V. Karpenka NAN Ukrayini (Development of fracture processes researches using the phenomenon of acoustic emission at H.V. Karpenko Physico-Mechanical Institute of the National Academy of Sciences of Ukraine). Preprint, NAN Ukrayini, Fizyko-mechanichniy institut, 1(2000), L'viv
79. Schnitt-Thomas KG, Stengel W (1983) Möglichkeiten zur Früherkennung von Wasserstoffschädigungen in metallischen Werkstoffen durch Anwendung der Schallemissionanalyse. *Werkst Korros* 34:7–13
80. Andreykiv AY et al (1990) Zastosuvannya metodu akustichnoyi emisiyi pry doslidzhenni materialiv u vodnevomu ta koroziynomu seredovischach (Application of the method of acoustic emission for investigation of materials in hydrogen and corrosive environments). *Fizyko-chimichna mechanika materialiv* (Physicochem Mech Mater) 5:26–36
81. Andreykiv OY, Lysak MV, Skalsky VR (1996) A method of accelerated evaluation of K_{ISCC} under stress corrosion cracking. *Eng Fract Mech* 54(3):387–394
82. Andreykiv AY et al (1992) Metodika opredeleniya K_{ISCC} stali v srede vodoroda s pomosh'yu metoda akusticheskoy emissii (A method of determining K_{ISCC} values of steel in hydrogen using acoustic emission). *Tekhnicheskaya Diagnostika i Nerazrushyushchii kontrol* (Tech Diagn Nondestr Test) 1:18–26
83. Skalskiy VR (1995) Vliyanie vodoroda na rastreskivanie metallov i kontrol' takikh prozessov metodom AE (Influence of hydrogen on metal cracking and testing of such processes by AE method). *Ibid* 1:52–65
84. Skalskiy VR, Andreykiv OYe, Serhiyenko OM (1999) Ozinka vodnevoyi poshkodzhenosti materialiv za amplitudamy signaliv akustichnoyi emisiyi (Estimation of hydrogen damaging of materials by acoustic emission signal amplitudes). *Ibid* 1:17–27
85. Hartbower CE, Gerberich WW, Crimmins PP (1967) Mechanisms of slow crack growth in high-strength steels. Aerojet-General Corporation, Sacramento, California. Feb 1967, vol 1, pp 213–245
86. Hartbower CE et al (1972) Use of acoustic emission for the detection of weld and stress-corrosion cracking. Acoustic emission, ASTM STP 505. American Society for Testing and Materials. Philadelphia, Pennsylvania, pp 187–221
87. Jaffrey D (1979) Sources of acoustic emission (AE) in metals. A review. *Non Destr Test (Aust)* 16(6):16–23

Acoustic Emission

Methodology and Application

Nazarchuk, Z.; Skalskyi, V.; Serhiyenko, O.

2017, XIV, 283 p. 144 illus., 3 illus. in color., Hardcover

ISBN: 978-3-319-49348-0